

ASSESSING PHENOLOGICAL CHANGES AND DRIVERS
IN EAST AFRICA FROM 1982 TO 2006

By

Chuan Qin

A THESIS

Submitted to
Michigan State University
in partial fulfillment of the requirements
for the degree of

MASTER OF SCIENCE

Geography

2011

ABSTRACT

ASSESSING PHENOLOGICAL CHANGES AND DRIVERS IN EAST AFRICA FROM 1982 TO 2006

By

Chuan Qin

Ecosystems in East Africa are undergoing changes due to climatic and anthropogenic factors. Plant phenology, an important ecosystem property and among the first to respond to climate change, is the focus of this thesis. Recent studies have shown that plant phenology is changing; however, they have not addressed causes of the changes. The objectives of this thesis are to examine how plant phenology has changed from 1982 to 2006 in East Africa using remotely sensed data and to identify the possible drivers behind observed phenological changes. Information extracted from time series remotely sensed imagery revealed a great variability in phenological patterns over East Africa. It was found that the phenological patterns were highly correlated with precipitation patterns and land cover types. Temporal trends were computed using Mann-Kendall test and Sen's slope method, and the results indicated there were significant phenological changes from 1982 to 2006 ($\alpha = 0.05$). The start of the growing season has delayed in large parts of Tanzania while been earlier in parts of Uganda. The length of the growing season has reduced in parts of Tanzania while lengthened in parts of Uganda. Phenological driver analysis was conducted at two hot-spots with significant phenological changes, to determine the relative importance of climatic factors and land use/cover changes. The results suggested that climate change is a dominant factor at one hotspot (Tarangire National Park, Tanzania). However, anthropogenic factors were found to be dominant at another hotspot (Tabora District, Tanzania). In conclusion, climatic and anthropogenic factors are important contributors to phenological changes but their degrees of influence differ from place to place.

ACKNOWLEDGMENTS

I would like to express my sincere gratitude to my advisor, Dr. Jiaguo Qi for his great support and guidance throughout my graduate program. His critical thinking and persistence in scientific research inspired me to complete this thesis. I am truly grateful for his encouragement, advice, and commitment. I also wish to thank Dr. Ashton Shortridge and Dr. Jennifer Olson for their assistance and encouragement to shape and improve my work from the very beginning of my study.

I sincerely thank the faculty and staff at the Department of Geography and Center for Global Change and Earth Observations for their guidance and support during my study. I would like to thank EACLIPSE project members I have worked with, Dr. David Campbell, Dr. Nathan Moore, Dr. Jeffrey Andresen, Dr. Gopal Alagarswamy, and Dr. Sarah Hession for being generous with their time and guidance. I am also grateful for the encouragement and help from my colleagues at CGCEO and fellow graduate students in the department. And lastly, I want to express my appreciation to my friend, Marsha Parrott-Boyle, for editing my thesis.

My deepest gratitude goes to my mother, my father, and my brother for unconditional love and continuous encouragement. Finally, from the bottom of my heart, I want to thank my fiancé, Xian. Without his support, understanding, and love, I would not have been able to complete this work.

Funding for this work was provided by the National Science Foundation Biocomplexity of Coupled Human and Natural Systems Program award BCS/CNH 0709671, entitled “Dynamic Interactions among People, Livestock, and Savanna Ecosystems under Climate Change”.

TABLE OF CONTENTS

LIST OF TABLES	vii
LIST OF FIGURES	viii
ABBREVIATIONS	x
Chapter 1 INTRODUCTION	1
Chapter 2 LITERATURE REVIEW	7
2.1 Plant Phenology: a brief introduction.....	7
2.2 Phenological Response to Climate Change.....	11
2.3 Remote Sensing Approaches.....	14
Chapter 3 STUDY AREA and METHODS	17
3.1 Over Research Design.....	17
3.2 Study Area.....	18
3.3 Data	21
3.3.1 GIMMS NDVI products	22
3.3.2 MODIS EVI products	23
3.3.3 Climatic data	24
3.3.4 LANDSAT data	25
3.3.5 Land cover products.....	26
3.4 Phenological Attributes Extraction	27
3.5 Spatial Variation Analysis.....	31
3.6 Temporal Trend Analysis.....	31
3.7 Driver Analysis	33
3.7.1 Land cover change	33
3.7.2 Climatic factor	35
Chapter 4 RESULTS	36
4.1 Regional Phenological Attributes.....	36
4.1.1 Phenological patterns for different land cover types	36
4.1.2 Spatial variations of phenological variables	40
4.1.3 Phenological changes over time.....	46
4.1.3.1 Temporal trends at pixel level	46
4.1.3.2 Temporal shifts for whole study area	50
4.1.4 Regional changes in land cover and annual precipitation.....	56
4.2 Local Scale Understandings	58
4.2.1 Tarangire National Park, Tanzania (Site I)	59
4.2.2 Tabora District, Tanzania (Site II)	66
Chapter 5 DISCUSSION and CONCLUSIONS	72

REFERENCES	77
------------------	----

LIST OF TABLES

Table 3-1. Land cover types used in TM/ETM classification	34
Table 4-1. Land use/cover change for East Africa (1992 - 2004)	57
Table 4-2. Land cover change matrix for site I (1985 - 2000).....	66
Table 4-3. Land cover change matrix for site II (1985 - 2003)	70

LIST OF FIGURES

Figure 3-1. Flow chart of research design	17
Figure 3-2. a) Overview of study area extent; b) Administrative boundaries inside the study area	18
Figure 3-3. Land cover map of study area based on GLC2000	20
Figure 3-4. Double logistic function example	29
Figure 3-5. Phenological variables extracted.....	30
Figure 4-1. NDVI profiles for typical land cover types in the study area	37
Figure 4-2. Spatial pattern of the start of growing season (SGS): SGS of Season 1 (left), SGS of Season 2 (right)	40
Figure 4-3. Spatial pattern of the end of growing season (EGS): EGS of Season 1 (left), EGS of Season 2 (right)	41
Figure 4-4. Spatial pattern of the length of growing season (LGS): LGS of Season 1 (left), LGS of Season 2 (middle), LGS of Season 1 + Season 2 (right)	42
Figure 4-5. Spatial pattern of the NDVI_Peak of growing season: NDVI_Peak of Season 1 (left), NDVI_Peak of Season 2 (right)	43
Figure 4-6. Spatial pattern of annual precipitation (Mean of 1982 -2006, CRU data)	44
Figure 4-7. Spatial pattern of the large (left) and small (right) integral of growing season	45
Figure 4-8. Maps of trends for phenological variables from 1982 to 2006: a, Start of Growing Season (SGS); b, End of Growing Season; c, Length of Growing Season; d, Large Integral; e, Small Integral.....	47
Figure 4-9. Histograms of whole study area for variable Start of Growing Season (SGS) shift between three time periods: 1982-1989, 1990-1999, 2000-2006. (a): Season 1; (b): Season 2. ..	51
Figure 4-10. Histograms of whole study area for variable End of Growing Season (EGS) shift between three time periods: 1982-1989, 1990-1999, 2000-2006. (a): Season 1; (b): Season 2. ..	53
Figure 4-11. Histograms of whole study area for variable Length of Growing Season (LGS) shift between three time periods: 1982-1989, 1990-1999, 2000-2006.	54
Figure 4-12. Histograms of whole study area for variable Large Integral of Growing Season (Lintegral) shift between three time periods: 1982-1989, 1990-1999, 2000-2006.....	55
Figure 4-13. Land cover maps of East Africa: 1992 (IGBP DISCover); 2004 (MOD12Q1).....	56

Figure 4-14. Map of trends for annual precipitation (CRU data: 1982 - 2006).....	58
Figure 4-15. Location of site I	59
Figure 4-16. Mean monthly rainfall at Monduli station (-3.32°S, 36.35°E) from 1981 to 2008 ..	60
Figure 4-17. Comparison between SGS and Total rainfall before SGS at site I	61
Figure 4-18. Comparison between the LGS and Rainfall_LGS; Lintegral and Rainfall_Lintegral at site I.....	62
Figure 4-19. Results from GIMMS data against results from MODIS data.....	64
Figure 4-20. Land cover classification maps (based on Landsat images) of site I in January, 1985 and February, 2000	65
Figure 4-21. Location of site II.....	67
Figure 4-22. Comparison between SGS and Total rainfall before SGS at site II	68
Figure 4-23. Comparison between the LGS and Rainfall_LGS; Lintegral and Rainfall_Lintegral at site II	69
Figure 4-24. Land cover classification maps (based on Landsat images) of site II in March, 1985 and May, 2003	70

ABBREVIATIONS

AVHRR	Advanced Very High Resolution Radiometer
CRU	Climatic Research Unit
EGS	End of growing season
ENSO	El Niño/La Niña-Southern Oscillation
ETM+	Enhanced Thematic Mapper Plus
EVI	Enhanced Vegetation Index
GIMMS	Global Inventory Modeling and Mapping Studies
GLC2000	Global Land Cover 2000
ITCZ	Intertropical Convergence Zone
LGS	Length of growing season
Lintegral	Large Integral
MODIS	Moderate Resolution Imaging Spectroradiometer
NDVI	Normalized Difference Vegetation Index
NOAA	National Oceanic and Atmospheric Administration
SGS	Start of growing season
Sintegral	Small Integral
TM	Thematic Mapper

Chapter 1 INTRODUCTION

Levels of greenhouse gases in the atmosphere have increased since large-scale industrialization around 150 years ago (IPCC 2007). The rising concentrations of greenhouse gas generally have triggered changes in modern climate. The most obvious and easily measured change is in global average surface temperature (IPCC 2007). The temperature has increased by $0.65^{\circ}\text{C} \pm 0.2^{\circ}\text{C}$ over the period from 1901 to 2005 (IPCC 2007), and the rate of warming since the 1970s was twice the rate for the whole period. Global temperature is also projected to continue rising rapidly if there are no effective controls on carbon emission. The world hydrological cycle has also been altered, resulting changes in precipitation patterns, including amount, frequency, intensity, and duration (IPCC 2007, Trenberth et al. 2003). Significant changes in annual precipitation from 1900 to 2005 have been observed in many places. For example, precipitation has increased in North and South America, northern Europe, and northern Asia, but decreased in parts of Africa and southern Asia. In addition, the frequency and variability of extreme events associated with temperature, precipitation, tropical and extra-tropical cyclones and severe local weather events have also changed in the 20th century, especially since 1979 (IPCC 2007). Climate change also has consequences in other aspects, such as rising sea levels, melting glaciers, risk to human health, and changing ecosystems.

Among these consequences, effects of climate change on plants are of particular importance because plants are the basis of global food production and a key factor in the global carbon cycle. The absorption of carbon dioxide during photosynthesis is the major pathway by which carbon is removed from the atmosphere and made available to animals and humans for growth and development. As carbon dioxide (CO₂) is the principle greenhouse gas, plants have clearly played an important role in mitigating climate change influences. In addition, plants are

major direct or indirect sources of food for human beings and also provide other useful non-food products like lumbers. However, plants have been affected by recent changes in climatic variables, such as CO₂ concentration, temperature, and precipitation. The most direct response is change in plant productivity. Generally increased levels of CO₂ in the atmosphere can generally increase plant productivity, so long as no other factors such as water are limiting. Increased temperature can also increase plant growth rate. However, the productivity could also be affected by negative consequences brought on by climate change, such as increased damage from insects and diseases. At the ecosystem level, climate change causes changes in plant diversity: plants are adapting to new environments, migrating to other places with suitable conditions, or just going extinct. In conclusion, impact on plants is a critical factor which should be carefully examined in the context of recent climate change as it is so vital to the natural ecosystem and human society.

There are many interesting study domains, including plant morphology, ecology, and physiology. But plant phenology, a study of seasonal life cycle events (Lieth 1974), is among the first responses at individual and ecosystem levels to climate change (Badeck et al. 2004). For plants, the seasonal timing of such events can be critical to survival and reproduction. And it has been shown that phenology plays a crucial role in multiple systems: the carbon balance of terrestrial ecosystems; geographic shifts in vegetation zones; vegetation-induced feedback to the atmospheric boundary layer; ecosystem biodiversity (Cleland et al. 2007, Foley et al. 1996, Keeling et al. 1996). The life stages of plants can be regulated by seasonal climate changes, including variations in temperature, precipitation, and photoperiod (Badeck et al. 2004, Estrella et al. 2007, Peñuelas et al. 2009, Yang and Rudolf 2010). Thus it is important to document phenological events, such as bud burst, leaf flowering, and leaf senescence, and determine how

they are involved with the seasonal climatic changes because it offers evidence of climate change happening now and helps in estimating future impacts of climate change on plants.

Currently, numerous studies have reported that plant phenology has been affected by climate change. Studies in mid and higher latitudes have shown that the timing of spring events, including budburst and flowering, has been advanced particularly since 1970s, mainly due to global warming (Menzel 2000, Menzel et al. 2006, Parmesan and Yohe 2003, Root et al. 2003, Schwartz et al. 2006). The timing of autumn events, such as leaf senescence, was also observed to be later over Europe (Defila and Clot 2001, Menzel 2000, Stockli and Vidale 2004). Longer growing seasons have been detected in the northern hemisphere (Menzel 2000, Stockli and Vidale 2004, Zhou et al. 2001). In tropical areas, plant phenology has been shown to be more sensitive to precipitation than to temperature and photoperiod (Botta et al. 2000). Biomass production has been found to be increasing in parts of Sahel since the 1980s (Heumann et al. 2007, Seaquist et al. 2006).

Reports of ground-measured plant phenology dating to the 18th century have been studied (Defila 2001, Menzel 2000, Parmesan and Yohe 2003, Roetzer et al. 2000, Root et al. 2003). However, increasing interest requires analysis at larger spatial scales and over a longer time period. Because remotely sensed data have temporal and spatial resolution and derived vegetation indices which present vegetation productivity well, lots of studies have examined plant phenology using remotely sensed data (Boschetti et al. 2009, Justice et al. 1985, Myneni et al. 1997, Stöckli et al. 2004, Zhang et al. 2003, Zhou et al. 2001). Time series of remotely sensed data, for example, have been used to estimate the relationship between vegetation dynamics and temperature variations during past decades (Myneni et al. 1997, Zhou et al. 2001). In recent years, a number of different methods have been developed to extract specific important date of

phenological events, including pre-defined thresholds (Lloyd 1990, White et al. 1997), the backward-looking moving average (Reed et al. 1994), the largest NDVI increase (Kaduk and Heimarm 1996), and curve fitting (Jönsson and Eklundh 2004, Sellers et al. 1994, Zhang et al. 2003). Remotely sensed data also makes it possible to analyze the spatial variations of phenology at both regional and local scales (Li et al. 2010, Maignan et al. 2008, Moulin et al. 1997, Zhang et al. 2003, Zhang et al. 2004). More importantly, time series of vegetation indices data provides opportunities to examine changes of plant phenology under recent climatic changes. For example, Stöckli and Vidale (2004) checked the trends in phenological variables from 1982 to 2001 in Europe, such as spring date and autumn date using linear regression analysis and negative trends for spring dates and positive for autumn dates were observed. Chen et al. (2005) found apparent delay in growing season end dates and insignificant leaf senescence in eastern China using AVHRR NDVI data. Boschetti et al. (2009) derived key phenological stages for rice crops in northern Italy such as emergence and heading from MODIS data and found earlier leaf senescence from 2001 to 2005. Olsson et al. (2005) and Heumann et al. (2007) found increased growing season length and productivity in the Sahel region since the 1980s.

Given this body of global evidence, one fundamental question can be asked: why are these phenological changes happening? First, plant phenology is very sensitive to climate variations. Separate or integrated changes in climatic variables such as temperature and precipitation would result in phenological changes. On the other hand, because the changes were derived from remotely sensed data, land cover changes may also contribute to observed phenological changes. Unfortunately, as most of the efforts (Boschetti et al. 2009, Chen et al. 2005, Heumann et al. 2007) look at phenological changes employing remotely sensed data, the important drivers behind these phenological changes were not carefully discussed in previous

research. Thus my thesis will examine phenological changes during recent decades, and further previous research through focusing on identifying the forces driving these changes and their relative importance.

I chose a portion of East Africa as my study region as it is among the most vulnerable regions to the impacts of climate change (IPCC 2007) because of the lack of economic development and institutional capacity. Similar to those of other continents, the temperature of Africa has increased 0.7 °C over the 20th century (Hulme et al. 2001, IPCC 2007). Warming sea temperature is thought to be responsible for more frequent and more intense extreme weather events in Africa, such as heavy rain storms, flooding, fires, hurricanes, tropical storms and ENSO events (Funk et al. 2005, IPCC 2007). Interannual rainfall variability is high over most parts of Africa. The northern part of East Africa is experiencing increasing rainfall while the southern part is experiencing declining rainfall amounts (Schreck and Semazzi 2004). Anticipated changes will not be uniform throughout the year. For example, Hulme et al. (2001) suggest that under intermediate warming scenarios, parts of equatorial East Africa will likely experience 5-20% increased rainfall from December-February and 5-10% decreased rainfall from June-August by 2050. In addition, these changes are more likely to happen in the form of unpredictable weather events. For instance, there may be increased precipitation during the already wet season, thereby increasing chances of floods, while less precipitation will occur in the already dry season which will result in more frequent droughts and increased desertification (IPCC 2007). These climatic changes threaten the ecosystems and human livelihoods in East Africa. Agriculture, including crop and livestock agriculture, is critical to local livelihoods. However, crop yield and feed resources for livestock are highly affected by changes in temperature and especially precipitation (Funk et al. 2005). In similar ways, large populations of

wild animals are threatened as the plants they dependent upon could also readily be influenced. Current constraints in East Africa, such as widespread poverty, poor soil fertility, pests, and diseases, are aggravated by negative impacts from climate change. On the other hand, local land use practices, such as crop cultivation, heavy grazing, firewood extraction, are also coupled with climate change.

The objectives of this thesis are to examine how plant phenology has changed from 1982 to 2006 in East Africa using remotely sensed data and to identify possible drivers behind the observed phenological changes. Specific research questions are addressed:

- 1) What are the spatial variations of phenological variables over East Africa?
- 2) Have there been changes for phenological variables from 1982 to 2006? If so, how have they changed? What are the spatial variations of these changes?
- 3) What are the possible drivers of the phenological changes and their relative importance at some hotspots, considering the climatic and anthropogenic factors?

Chapter 2 LITERATURE REVIEW

Section 2.1 reviews the studies about the plant phenology, states the importance of vegetation phenology, and surveys the relationship between the vegetation phenology and the environment factors (temperature, rainfall, photoperiod, soil moisture, etc.). Section 2.2 summarizes studies focused on impacts of climate change on the ecosystem and how phenology responds to climate variations, such as changes in temperature and precipitation. Section 2.3 introduces the remote sensing approaches which have been developed to investigate plant phenology.

2.1 Plant Phenology: a brief introduction

Phenology is defined by Lieth (1974) as 'the study of the timing of recurrent biological events, the causes of their timing with regard to biotic and abiotic forces, and the interrelation among phases of the same or different species'. Plant phenology specifically is the study of the periodic events in the annual cycles of the vegetation, such as the onset of the green up.

Plant phenology determines the timing and growing cycle of all plants, thus it is critical to who depend on plants for food, including human beings and wild animals. Plant phenology also plays an important role in the disease control as the growth stages of insects and plants are correlated. For instance, desert locust breeding and migratory patterns are shown to be influenced by vegetation distribution and growth across the African desert (Despland et al. 2004). In addition to its role in biological lifecycles, plant phenology is also important in the terrestrial carbon cycle. Seasonal variations of CO₂ exchange has been found highly related with the seasonal shifts in vegetation photosynthetic activities (Aurela et al. 2001, Foley et al. 1996, Keeling et al. 1996, Lafleur et al. 2001). The plant phenology is connected to the CO₂ exchange

fluctuation: the CO₂ is released into the atmosphere after the leaf senesces while it is absorbed after the leaf green up. Plant phenology is also important in vegetation feedback to atmospheric boundary layer as changes in vegetation cover can modify the physical properties of land surface (Freedman et al. 2001, Foley et al. 2000). Consequently, knowledge of the phenology of plant communities is relevant to estimating biological productivity, understanding land-atmosphere interactions and biome dynamics, modeling vegetative inputs into biogeochemical cycles, as well as for the management of vegetation resources.

The major phenological patterns of plants, such as leafing, flowering, and fruiting have been found to be related with a variety of factors, such as rainfall, temperature, day length, soil moisture, and irradiance (Brooke et al. 1996, Fenner 1998, Lieberman and Lieberman 1984, Wright and Van Schaik 1994). Irradiance is believed to play an important role when other factors are not limiting. For example, the leaf and flowering production were found to coincide with peaks of irradiance (Fenner 1998, Wright and Van Schaik 1994). Photoperiod (day length) may also be determinant for leaf/flower timings. For example, Partanen et al. (1998) have found that the thermal time required for bud burst could be significantly reduced through long photoperiods.

Temperature also drives plant phenology as it is closely related to rates of chemical reactions, fluidity of membranes, and enzyme activities (Badeck et al. 2004). Typical timing of spring growth phases, like budding, leafing, and flowering of plants, is primarily triggered when accumulated temperature is above a threshold value (Beaubien and Freeland 2000, Fenner 1998). Partanen et al. (1998) also found that higher temperature can hasten the green onset. So in temperate regions where annual changes in temperature are dominant, vegetation growth cycles often correspond to the temperature pattern (Schwartz 1998). In arid/semi-arid zones, for most water limited species, precipitation is a major factor determining the phenological patterns. The

emergence of green leaves and vegetation growth duration are primarily controlled by precipitation in arid and semiarid ecosystems (Rodriguez-Iturbe et al. 1999a, 1999b). The growing of plants is strongly coupled to rainfall seasonality in seasonal climate regions (Kramer et al. 2000, Reich 1995, Zhang et al. 2005). But the phenology may also be affected by human activities, for example, leafing can be artificially induced by irrigation other than the natural precipitation. The properties of soil are also playing an important role in determining the phenological patterns of vegetation because whether the water can penetrate the soil quickly is a critical determinant for vegetation's response to rainfall. Vegetation, especially herbaceous species, grows rapidly and early on sandy soils since rainfall can quickly infiltrate and be available for plant growth. In contrast, a large amount of rainfall evaporates or runs off from clay soils with low infiltration rates (Rietkerk et al. 2000). Moreover, crusts developed on clay-dominated soils can significantly reduce infiltration, increase overland flow, and decrease soil moisture in the root zone (Casenave and Valentin 1992). In general, the onset of vegetation green-up occurs later and requires more precipitation in clay soils. Similarly, vegetation can grow longer in soils with high water retention. In addition to the above climatic drivers, other factors, such as disease, herbivore consumption, insect, fire, land degradation can also affect the vegetation dynamics.

The East Africa savanna has two major components: grass and wood. The phenological characteristics of them under arid/semi-arid climate in this region are worthy of interest. The start of growth of grasses depends on the occurrence of the first significant rain (Chidumayo 1994). And the grass greenness usually lasts for a relatively short period of time. So the sites with grass will appear barren again just several months after the rains. For example, a study in Tanzania (Prins 1988) found that grasses which seeds after an accumulated rainfall total of about

400mm during the middle of the long rains in April have a very short growing season, and eventually there was no green leaves left approximately in mid June. Different from the grasses, the woody components always start shooting in the dry season (maybe one to three months before the start of the rainy season), flowering largely occurs in the dry season, allowing fruit-set and dispersal in the rains (Chidumayo 1994). Thus most growth concentrates in wet season and peak green biomass occurred any time in wet rainy season (Dye and Walker 1987). Generally, the growth patterns of both grass and wood are highly coupled with the precipitation patterns. As to the soil moisture, the growth of grasses is especially restricted by soil water availability, except for those on floodplains and swamps, because grasses with dense and shallow root systems make use of water that is available in the upper layer of the soil (Scanlon et al. 2002). So the growth peaks of grasses usually occur in the rainy season (Prince and Tucker 1986). However, trees have a more persistent supply of soil water because of the root systems that can reach deeper soil layers (Scanlon et al. 2002), thus the leafing of trees is less dependent on the timing of rainfall. Another important vegetation type is crop. Crop phenology also depends upon environmental factors, including photoperiod, temperature, and precipitation. For example, the flowering date of rice is determined by genotype, photoperiod, and micrometeorology, and rainfall is important for crop maturation or harvest (Dingkuhn 1995). But it is also affected by crop management. For instance, rainfall is of minor importance in an irrigated system and cultivators determine the sowing date (Dingkuhn and Asch 1999).

In general, phenological characteristics of plants are closely related to those climatic factors. Changes in the climatic factor trigger corresponding changes in the phenology. As mentioned above, changes in phenological events are of great importance to crop management, global carbon cycle, and so on, thus studying phenological changes is very necessary.

2.2 Phenological Response to Climate Change

During the last century, global climate has been going through a lot of changes (IPCC 2007). The changes are expressing themselves in many ways: increasing atmospheric CO₂ concentration; increasing global average temperature; changing precipitation patterns; rising sea level; increasing extreme events, etc. The ecosystem is responding to such changes (Hulme 2005, King 2005, Parmesan and Yohe 2003, Root et al. 2003). At the species level, the growth cycle, or even existence of plants are affected. For example, increased CO₂ can increase photosynthesis and reduce water use of plants, and increased temperature can accelerate the growth rate of plants, advance the spring onset, and reduce frost days. At the ecosystem level, species distribution and abundance have been changed. For example, rising sea level could cause loss of land and coastal habitats; increased temperature and CO₂ concentration probably can cause geographical shifts in vegetation zones as well as species diversity. For instance, Parmesan and Yohe (2003)'s global meta-analysis found significant range shifts towards the poles at the speed of averaging 6.1 km per decade. Bond and Midgley (2000) and Bond et al. (2003) found that the ratio of herbaceous and woody components of African savannas is changing because of increasing atmospheric CO₂ concentrations. Plant phenology is essential for species coexistence in the ecosystem because of the variation among species in their phenology which reduces the competition for resources (Cleland et al. 2007). Therefore, plant phenology is of great importance to the ecosystem. And as plant phenology can be regulated by changes in climate, numerous researches have studied changes in plant phenology in the context of global climate change.

Increased CO₂ concentration is one of the most important expressions of global change. Although increasing CO₂ level can increase photosynthesis activities generally, the potential direct effect of CO₂ enrichment on the plant phenology is still not clear (Badeck et al. 2004). Most researches have focused on other climatic factors, such as temperature and precipitation.

Over the past 30 years, global average surface temperatures were found to increase by 0.28 °C per decade. Therefore, lots of studies have been conducted to study how phenology changed according to the increases in temperatures (Chen et al. 2005, Menzel 2000, Menzel et al. 2006, Parmesan and Yohe 2003, Root et al. 2003, Stockli and Vidale 2004, White et al. 1999, Zhou et al. 2001). Their research has showed earlier onsets of spring events due to the rising temperature in Europe (Menzel 2000, Menzel et al. 2006, Stockli and Vidale 2004), North America (Bradley et al. 1999, Schwartz et al. 2006, White et al. 1999, Zhou et al. 2001), and Asia (Chen et al. 2005, Corlett and Lafrankie 1998). Nevertheless, the timing of autumn events, such as leaf essence, has shown both delayed and earlier trends (Defila and Clot 2001, Menzel 2000, Stockli and Vidale 2004) over the same time period. Longer growing seasons have been detected in many parts of Northern hemisphere (Chen et al. 2005, Menzel 2000, Zhou et al. 2001). Even at a much smaller scale, temperature difference induced by human in rural and urban areas can result in differences in phenology. The start of the growing season of urban areas is earlier than the adjacent natural vegetation due to the heat island effects (Zhang et al. 2004).

Although temperature and photoperiod control phenology in the high latitudes, for tropical systems like semiarid savannas, precipitation is the main driving force in deciding the vegetation composition and distribution (Rodriguez-Iturbe et al. 1999a, 1999b). The seasonality of rainfall has the most significant impact on structure and function of these systems. Thus,

phenology in this region is very sensitive to the global climate change through the modification of rainfall seasonality, and the occurrence of extreme weather events (floods and droughts).

The timing of precipitation is very vital to most plants. For example, miombo woodlands would be vulnerable to late spring rainfall (Fuller et al. 1996). Earlier green onsets were found in parts of West and Southern Africa largely because of earlier arrival of spring rainfall (Fuller et al. 1996, Heumann et al. 2007). A strong increase in vegetation growth amplitude and amount was detected in Sahel region due to increasing precipitation during 1982 - 1999 (Eklundh and Olsson 2003, Hickler et al. 2005).

For areas where precipitation patterns are strongly influenced by the El Niño Southern Oscillation (ENSO), the frequency and intensity of El Niño events are expected to increase due to rising sea temperature, and consequently influence the plant in these areas (Indeje et al. 2000, Nicholson and Kim 1997). As El Niño events are associated with wetter than normal conditions in rainy seasons, La Niña events are linked to prolonged drier conditions than normal in dry seasons of East Africa. These shifts in the timing and duration of the rainy season will directly affect the phenological pattern in East African countries. For example, prolonged and strong ENSO episodes associated with rising temperature and declining rainfall throughout the 1990s and early 2000s have caused large reduction in plant productions in the Mara-Serengeti ecosystem of Kenya and Tanzania (Ogutu et al. 2008).

In conclusion, in mid and high latitude regions, major climate components, especially the temperature is dominating the variability of plant phenology (Menzel 2000). Increasing temperature generally advances the timing of the spring phenology in the context of global warming (Parmesan and Yohe 2003, Root et al. 2003). In tropical areas where biome is water-

limited, precipitation is accounting for phenology variability. The changes in precipitation patterns, including intensity, duration, and extreme events, are affecting the plant phenology.

2.3 Remote Sensing Approaches

Historic records of phenological events provided detailed long term records for phenology study (Parmesan and Yohe 2003, Root et al. 2003). However, they are not sufficient because they usually focused on individual community or individual species at local scales. Ground observation data cannot meet the data requirement for phenology over a large area. Thus, with global coverage, remotely sensed data has been introduced to phenology studies. The capacity of satellite sensors to detect important phenological events such as leafing and flowering is limited due to the ground resolution of the sensors, the effects of other vegetation, and soil background characteristics. While limited in some aspects, satellite sensors are still capable of measuring broad-scale changes in the landscape that may not be associated with phenological events of specific plants, but are descriptive of ecosystem conditions (Reed et al. 1994).

Vegetation indices (VI), such as Normalized Difference Vegetation Index (NDVI) and Enhanced Vegetation Index (EVI) offered an objective way of evaluating phenological characteristics and assessing their spatial variability over large geographic areas (Justice et al. 1985). Vegetation indices derived from remotely sensed data have been frequently used in research on vegetation ‘greenness’ or productivity as it minimizes soil and other background effects, reduces data dimensionality, and provides a degree of standardization for comparison. The evolution of the vegetation index through time, exhibits a strong correlation with the typical green vegetation growth stages (emergence, vigor/growth, maturity, and harvest/senescence)

(Justice et al. 1985). Thus VI time-series provides an effective way to observe phenological attributes, such as start of season, end of season, length of growing season, etc.

After VI time series have been introduced, a variety of methods have been developed to extract the phenological metrics from VI time-series. Lloyd (1990) proposed to set a threshold value at which vegetation begin to grow. However, the absolute growth varies with vegetation type, soil background, and illumination conditions. Therefore, it is not possible to establish a single and effective threshold for various cover types in different environment backgrounds. Reed et al. (1994) proposed backward-looking moving averages method which determines the onset of greenness when the NDVI exhibits a sudden increase. Sellers et al. (1994) applied Fourier smoothing by fitting the first three harmonics through the data with a least squares method. White et al. (1997) integrated the basic concepts of traditional meteorologically based phenology modeling with intensive satellite phenological observations and produced biome-specific ecosystem phenological models. Zhang et al. (2003) utilized a series of piecewise logistic function to fit to the MODIS NDVI time-series. Jönsson and Eklundh (2004) have implemented three methods in TIMESAT program which is designed to analyze time-series satellite data: adaptive Savitzky–Golay filter, asymmetrical Gaussian and double logistic. The idea of curve fitting is very useful as this processing is based on individual pixel without setting thresholds or empirical constants, which makes the method globally applicable. Furthermore, it is flexible. It can identify multiple growing periods in one year, which is particularly important for tropical regions or irrigated crops.

Although remotely sensed data has been frequently used to study the phenology, some potential problems must be kept in mind. Firstly, satellite signals might be biased. They may be affected by several sources of noise, such as the effects of the atmosphere, the instability of

sensor response, and satellites orbit. Secondly, due to the spatial resolution issue, a satellite observation pixel is mixed. One pixel does not represent only one plant type. Instead, most times it is a mixture of whatever intersected the sensor's field of view. Thus the phenology observed from remote sensing data is only proximity of the physical phenology.

Chapter 3 STUDY AREA and METHODS

3.1 Over Research Design

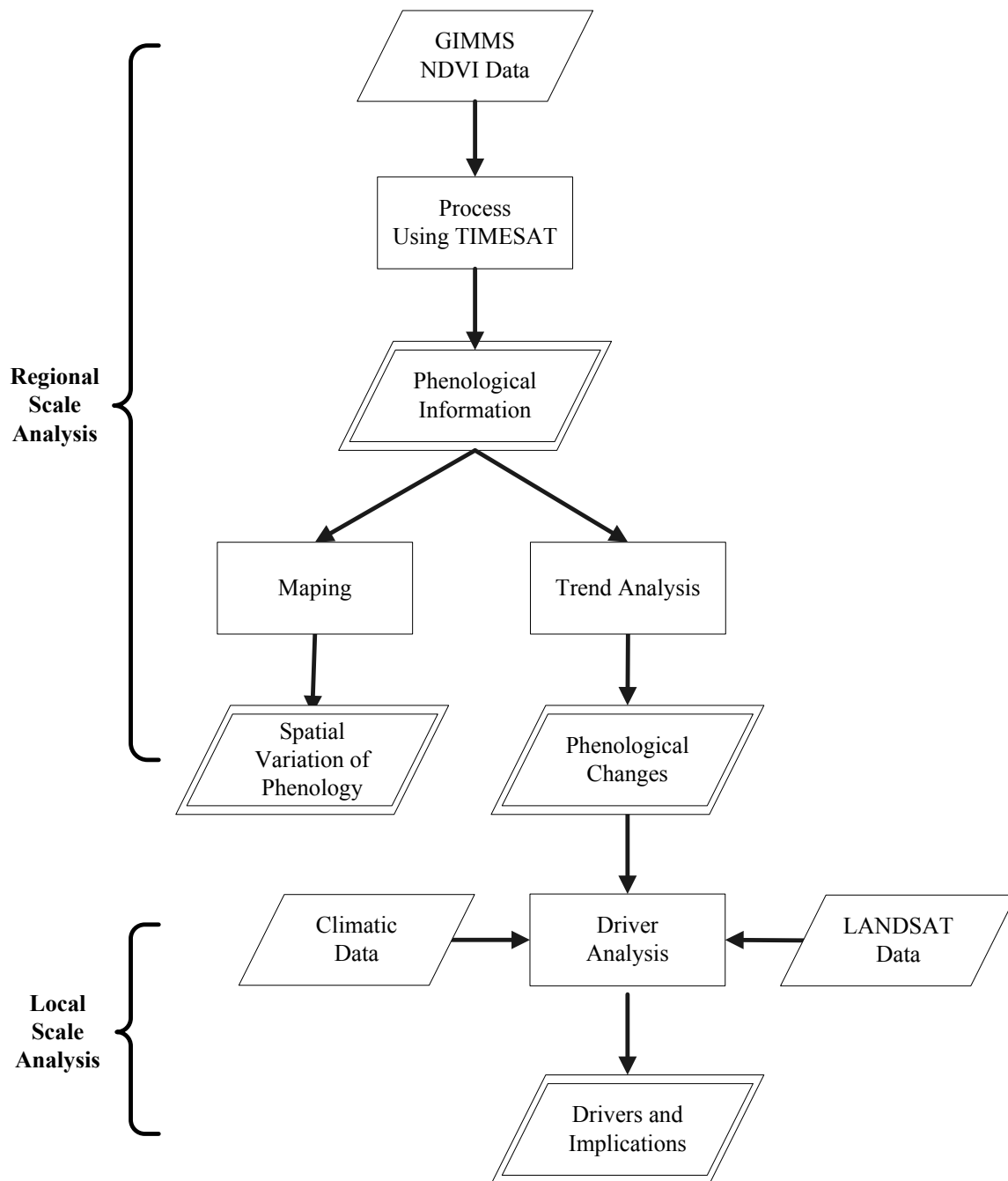


Figure 3-1. Flow chart of research design

At the regional scale, the phenological information was extracted from GIMMS NDVI time series spanning from 1982 to 2006. Then spatial patterns of each phenological variable were

examined. How the phenology has changed during this period was also checked using temporal trend analysis. At the local scale, hotspots with significant phenological changes were selected and looked into the drives of phenological changes in terms of climatic and land cover factors.

3.2 Study Area

In this thesis, East Africa is defined as the area between latitude 5° N and 12° S, and longitude 28°E and 42°E. East Africa region is comprised of countries, including Kenya, Uganda, Tanzania, Rwanda, and Burundi (Figure 3-2).

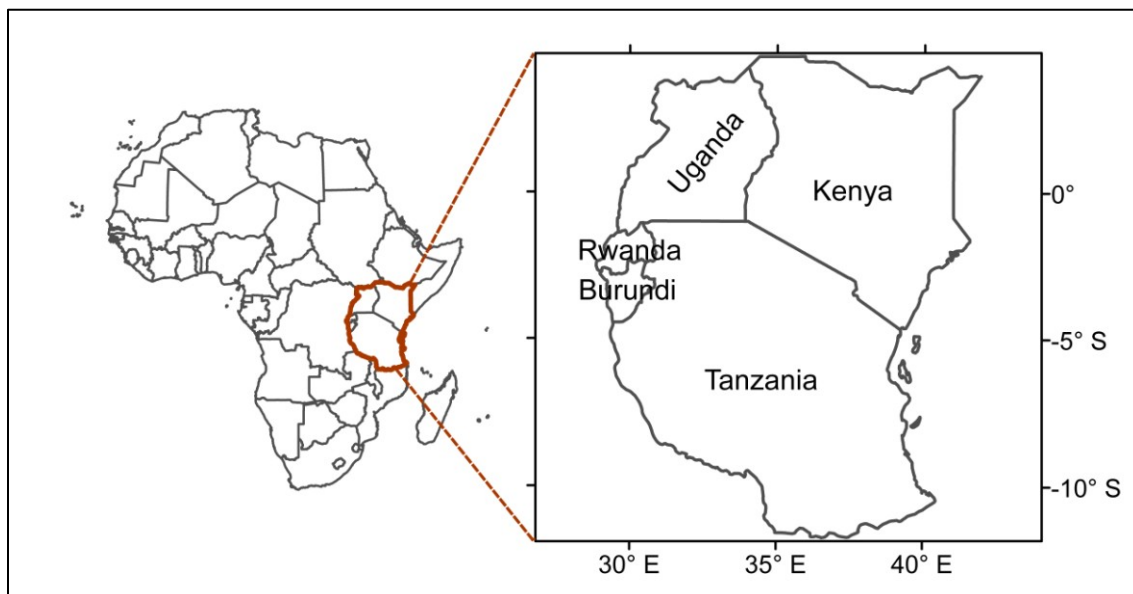


Figure 3-2. Overview of study area extent
(For interpretation of the references to color in this and all other figures, the reader is referred to the electronic version of this thesis.)

Temperatures in East Africa are generally moderate throughout the year and little variation occurs during the year (McClanahan and Young 1996, IPCC 2007). The annual rainfall is spatially heterogeneous. The areas with the most rainfall are those with longest rainy seasons, e.g., the northwest of Lake Victoria, the highest relief areas surrounding Mt. Kenya and Mt.

Kilimanjaro, and the southeast of Tanzania. Driest regions are in the north of Kenya, where mean annual rainfall is generally less than 400mm. In the desert core, it is around 200mm. Most Uganda has abundant rainfall exceeding 1000mm. Over most of Tanzania, mean annual rainfall is on the order of 800 to 1200mm. There is also a pattern of decreasing rainfall from the west to the east in south hemisphere due to the expansion of the low pressure wet air from central Africa (McClanahan and Young 1996).

The rainfall pattern also has significant spatial variations. The equatorial region, including Kenya, south Uganda, and north Tanzania, experiences a bimodal seasonal distribution of rainfall, with maxima occurring in the two transition seasons. In regions like southern, south-west, central and western parts of Tanzania, the seasonality is more unimodal, with the maximum occurring during the high-sun season of the hemisphere. The dominant precipitation pattern is a seasonal north to south movement of the main rain belt, a consequence of the dominant influence of the Intertropical Convergence Zone (ITCZ). In equatorial bimodal regions, heavier rains occur from March to May which is called 'long rains' and less rain happens in October to November which is called 'short rains'. From June to September, this region is nearly rainless except for an area around Lake Victoria and a small strip around the coast. In the southern and northern unimodal regions, there is only single rainfall peak. For instance, in southern Tanzania, heavy rainfall occurs from December to April (McClanahan and Young 1996).

Over the past 30 years, East Africa has experienced at least one major drought in each decade. There were serious droughts in 1973/74, 1984/85, 1987, 1992-1994, and in 1999/2000. By contrast, at some years, the region has experienced above-average rainfall, such as 1997.

Projections of climate change also suggest that East Africa will experience more droughts and erratic rains in the future (Hulme et al. 2001, IPCC 2007).

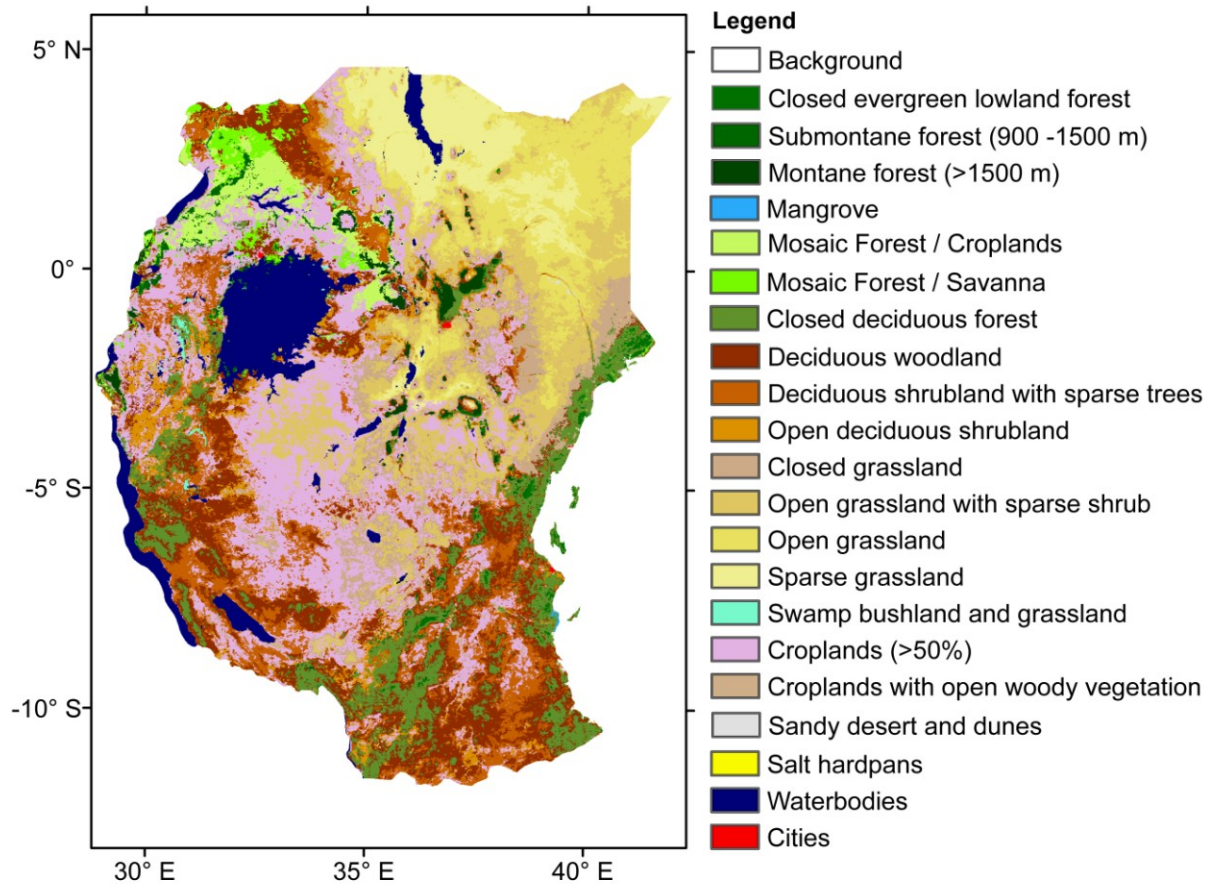


Figure 3-3. Land cover map of study area based on GLC2000

There are various vegetation types in East Africa, which often varied with water availability and altitudes. Forest are located along the coasts, on the high mountains, and scattered in some other places, such as the riverside. Evergreen broadleaf forests are located in the Congo Basin, northern of Lake Victoria, and peaks of high mountains. Deciduous broadleaf forests are mainly located on the coast. Savanna is characterized by the coexistence of grasses and trees (McClanahan and Young 1996). And the chief characteristic is recognized to be the dominance of grasses in the understory, while the height and spacing of the trees and shrub

component determine the categories of the savanna. The savannas spread into the areas with an average rainfall less than 600mm and two rainfall seasons, including Kenya, northern Tanzania, and northeast Uganda. Miombo woodland is another typical land cover types in East Africa. These deciduous woodlands are in areas with a single rainfall peak, which most are in southern parts of East Africa. Sometimes, people also call miombo woodland ‘moist savanna’ because the rainfall in miombo areas is always higher than the savanna areas. There are also woodlands in southern Sudan with abundant rainfall. Croplands are located mainly along the Great Lakes, and in the highlands.

The vegetation is an important linkage between human, wildlife, and livestock. Wildlife depends on the herbaceous layer for food. For human, savannas provide lands for both agriculture and pasture for domestic herds. Human activities are also influencing as human-induced fire or grazing could reshape the savanna. As the ecosystem is sensitive to both human and climate disturbances, understanding how vegetation dynamics changed over recent decades and assessing the impacts of recent land-use changes or climate changes, are very important, in terms of understanding the ecology of the region, which is critical for both conservation and future development.

3.3 Data

In the large scale analysis, long term remotely sensed data were used to extract phenological parameters. In the zoomed in analysis, LANDSAT data were used to detect land cover changes because of its higher spatial resolution. And the climate related data, focused on precipitation, were applied to help understand the relationship between the phenology and climate changes.

3.3.1 GIMMS NDVI products

Long term NDVI (Normalized Difference Vegetation Index) time series is produced by the Global Inventory Modeling and Mapping Studies (GIMMS) group (Pinzon et al. 2005, Tucker et al. 2004, Tucker et al. 2005). It is derived from imagery obtained from the Advanced Very High Resolution Radiometer (AVHRR) instrument onboard the National Oceanic and Atmospheric Administration (NOAA) satellite series 7, 9, 11, 14, 16, and 17. NOAA AVHRR has provided global coverage since 1981 and has required temporal resolution to create time series. The GIMMS NDVI data are 15-day maximum-value composites for a 25 year period spanning from 1981 to 2006 and at 8 km spatial resolution.

The NDVI exploits the spectral properties of green plant leaves, which absorb incoming radiation in the visible part of the spectrum (AVHRR channel 1: 0.58 to 0.68 μm) and strongly reflect light in the near-infrared wavelengths (AVHRR channel 2: 0.73 to 1.1 μm). This ratio ($\text{NDVI} = (\text{NIR} - \text{RED}) / (\text{NIR} + \text{RED})$) has low values ranging from -0.2 to +0.1 for snow, bare soil, glaciers, rocks, and rises to around 0.2–0.8 for green vegetation. NDVI has been shown highly correlated with vegetation parameters such as green-leaf biomass and green-leaf area, and absorbed photosynthetically active radiation, and consequently variations from vegetation cover could result in changes in NDVI. However, there are also factors other than the actual vegetation cover that can cause variations in NDVI, such as seasonal variations in atmospheric water vapor, atmospheric aerosol content (Huete et al. 1997). Nevertheless, the NDVI is still the most broadly used to monitor vegetation dynamics in most terrestrial ecosystems (Chen et al. 2001, Studer et al. 2007).

There are actually other products from NOAA AVHRR, such as the PAL (Pathfinder AVHRR Land) dataset, but GIMMS dataset presents several improvements (Tucker et al. 2005, Pinzon et al. 2005). First of all, GIMMS presents a better data process, including correction for sensor differences, satellite sensor drift, view geometry, effects of major volcanic eruptions during the period. Furthermore, the GIMMS data is provided along with flags files, which indicate the quality of the NDVI, for instance, whether the data was obtained directly from satellite data, or if the data might correspond to snow. In addition, the GIMMS NDVI is presented as 15-day maximum-value composites which select the maximum NDVI value for each pixel from 15 days period. This compositing technique helps to minimize cloud cover, atmospheric and off-nadir viewing effects (Holben 1986) because pixels that have a lower NDVI value than expected when they are contaminated by some factors, such as cloud cover, atmospheric, and off-nadir effects, will be minimized by the compositing.

GIMMS NDVI data have been widely used in phenology studies (Heumann et al. 2007, Zoffoli et al. 2008) and the results have shown that the GIMMS NDVI data are able to capture general patterns of vegetation dynamics, and variations of vegetation signals.

3.3.2 *MODIS EVI products*

GIMMS NDVI dataset provides a very long term time series, spanning from 1982 to 2006, but the spatial resolution is coarse. The Moderate Resolution Imaging Spectroradiometer (MODIS) instrument on-board NASA's Terra and Aqua platforms can provide better spatial resolution (250 - 1000 m) but short term (2000 - present) time-series (Justice et al. 1998). I used the 16-day maximum composite MODIS EVI (Enhanced Vegetation Index) dataset at a 250m resolution spanning the period from 2000 to 2009 (the MOD13Q1 product, Huete et al. 2002).

The Enhanced Vegetation Index (EVI) is calculated from surface reflectance data corrected for molecular scattering, ozone absorption, and aerosols (Huete et al. 2002):

$$EVI = 2.5 \times \frac{NIR - RED}{NIR + 6 \times RED - 7.5 \times BLUE + 1} \quad (1)$$

The coefficients 2.5 and 1 represent the gain and canopy background, respectively (Huete et al. 2002). The coefficients 6 and 7.5 are representing the aerosol resistance term, which uses the blue band to correct for aerosol influences in the red band. The EVI is an improved vegetation index compared with NDVI, as it enhances the vegetation signal with improved sensitivity in high biomass regions and improved vegetation monitoring through eliminating canopy background signal and residual aerosol influences. Additionally, it solves the saturation problem in NDVI as it does not become saturated as easily as the NDVI. Similar with NDVI compositing, the MODIS is daily basis thus the data are composited into a 16-day maximum value product that reduces the potential effects of clouds or other atmospheric scatter.

With improved spectral, radiometric, and geometric corrections, MODIS data have offered an effective means of detecting phenological pattern and monitoring detailed vegetation dynamics (Zhang et al. 2003, Zhang et al. 2004).

3.3.3 Climatic data

The rainfall data used in this paper is Climatic Research Unit (CRU) TS 3.0 dataset (Mitchell et al. 2005) from East Anglia University. It is a gridded dataset, covering the global land surface at 0.5 degree resolution for the period 1901-2006. Nine climate variables are available: daily mean, minimum, and maximum temperature, diurnal temperature range, precipitation, wet day frequency, frost day frequency, vapour pressure, and cloud cover. Monthly

precipitation data from 1982 to 2006 was extracted for the study area (Latitude: 6° N ~ 15°S; Longitude: 27°E ~ 42°E).

Another source of rainfall data is from rainfall stations which were obtained from Department of Meteorology, Tanzania. The records include several climatic factors: total monthly precipitation, mean minimum temperature, and mean maximum temperature from about 17 stations during the period from 1970s to 2008.

3.3.4 *LANDSAT data*

To examine the land cover changes, high resolution remote sensing images were needed. Landsat is one of the most popular data sources for land cover monitoring. It is a series of Earth-observing satellite missions jointly managed by NASA and the U.S. Geological Survey since 1972. Landsat satellite orbits the Earth at an altitude of 705 km, according to a sun-synchronous, near-polar orbit with an inclination angle of 98.22° with respect to the Equator. The revisit time and hence maximal temporal resolution of the sensor is 16 days. Landsat 4 and 5 carried an improved design of the MSS and the Thematic Mapper (TM) sensor. The MSS has four broad spectral regions, while the TM has seven spectral bands. The spatial resolution of Landsat 4 and 5 TM is 30m for 6 bands (1-5, 7) and 120m for the thermal band (band 6). Landsat 7 was launched in 1999 and carried an improved sensor called Enhanced Thematic Mapper Plus (ETM+). The spectral bands range from the visible to the thermal infrared. The spatial resolution of Landsat-7 ETM+ is 30m, 15 m for the panchromatic band (0.5 to 90 μ m), and 60 m for the thermal band.

The availability of Landsat TM/ETM+ images for the study sites was searched on the USGS website at <http://glovis.usgs.gov/>. One criterion of selecting data is cloud free images. For

some area, if cloud free images were hard to get, then the cloud cover must be under 10%.

Another concern is the date when the image was acquired. To reduce the impacts of seasonal and phenological variation, the image pairs need to be in the same season or very close for all target areas, because image acquired in the growing season is very different from the image acquired in dormancy periods.

3.3.5 Land cover products

The Global Land Cover 2000 (GLC2000) data is produced by the European Joint Research Centre (JRC), provides consistent global land cover information for the year 2000. It is built primarily on SPOT VEGETATION daily 1km data acquired from November 1999 to December 2000 (Mayaux et al. 2003). The project not only provides global land cover map but also eighteen regional land cover map products. Furthermore, the land cover classification system (LCCS) produced by United Nations (UN) which has 27 land cover classes were applied to each map. The regional map of Africa was downloaded for free from <http://www-gem.jrc.it/glc2000>.

The MODIS Land Cover Product (MOD12Q1) was developed by Boston University and coordinated by MODIS Land Team from National Aeronautics and Space Administration (NASA). The product characterizes the global land cover, and provides different spatial resolution (1km or 500m) options and different classification schemes, such as IGBP (International Geosphere-Biosphere Programme) and UMD scheme. The 1km product in year 2004 with IGBP classification scheme was selected in this thesis. The data was downloaded from Land Processes Distributed Active Archive Center (LP DAAC).

The DISCover product was designed to meet the various global land cover needs of IGBP core science projects. It was coordinated by the IGBP-Data and Information System's (IGBP-DIS) Land Cover Working Group (LCWG). The product was processed from AVHRR maximum monthly NDVI composites for 1992 -1993. The data set has global coverage at 1km spatial resolution and in 17 classes IGBP scheme. This IGBP DISCover data can be accessed from http://webmap.ornl.gov/wcsdown/dataset.jsp?ds_id=930.

3.4 Phenological Attributes Extraction

This part introduces how to get useful phenological information from remotely sensed vegetation index time series. For example, each GIMMS NDVI image presents the NDVI values of each pixel at a specified time. As GIMMS dataset is 15-day maximum-value composites, there will be 2 images in each month and thus 24 images for each year. By extracting NDVI values at a pixel (j, k) in the array for consecutive times, a time-series y_1, y_2, \dots, y_N is obtained for this pixel. Through all the following steps, phenological parameters, such as the start of the growing season, can be extracted from the time series.

The first step is to remove those spikes and outliers in the NDVI time series. These noises may be caused by uncertainties during the data acquiring and processing. A median filter method was utilized here. If a NDVI value in the time-series is different from the left and right neighbors in time, and from the median in a window (length is 4 images) will be classified as an outlier and removed. The difference is measured in units of the standard deviation of the time-series. The threshold is set at 2 standard deviations.

Many methods have been developed to extract phenological parameters from NDVI time-series. Among them, fitting a curve to the time-series has been widely used because this method is processed through each pixel which it is more flexible and not limited by setting local

thresholds. The reason of curve fitting is that the original NDVI time series is not continuous which only has values at discrete times. Curve fitting makes it possible to estimate NDVI values at times where no NDVI observations exist. A series of piecewise functions can be applied to any time period, not confined by the calendar year.

Generally, a time-series t can be represented by (t_i, y_i) , $i=1,2,...,N$ where t is time; y is the NDVI value; N is number of total images. A function to define NDVI series is:

$$f(t) = c_1 r_1(t) + c_2 r_2(t) + \dots + c_m r_m(t) \quad (2)$$

where $c_i r_i(t)$ is a basis function defined before fitting. In order to get best values for c_i , the ordinary least square method is applied.

In most cases, the function is fit locally to data in appropriate intervals between the maxima and minima in the time-series where they have sustained NDVI increase or decrease trend. So before the time-series could be fit to the function, it is necessary to identify those periods. In this study, a harmonic function was fitted to the time-series:

$$f(t) = c_1 + c_2 \sin(\omega t) + c_3 \cos(\omega t) + c_4 \sin(2\omega t) + c_5 \cos(2\omega t) \quad (3)$$

where $\omega = 6\pi / N$, The first basis function determines the base level. The pairs of sine and cosine functions correspond to respectively one and two annual vegetation seasons. The position of maxima and minima will be identified from the fitted function.

After determining the interval for local model function, it is time to choose appropriate function. A variety of functions has been developed and can be used in the above equation, such as harmonic, Gaussians, logistic, or wavelets. The double logistic function was selected here. The equation of double logistic function is:

$$g(t; x_1, \dots, x_4) = \frac{1}{1 + \exp(\frac{x_1 - t}{x_2})} - \frac{1}{1 + \exp(\frac{x_3 - t}{x_4})} \quad (4)$$

where x_1 determines the position of the left inflection point, x_2 gives the rate of change.

Similarly x_3 is the position of the right inflection point while x_4 is the rate of change at this point.

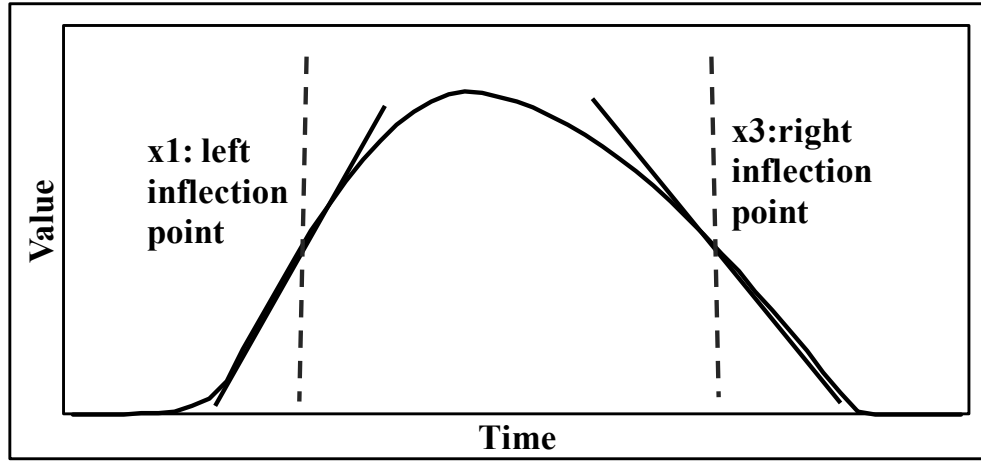


Figure 3-4. Double logistic function example

After the double logistic function has been fitted to the original NDVI time-series, a number of interesting phenological parameters can be extracted from the fitted function. The following figure is an example of the parameters extracted.

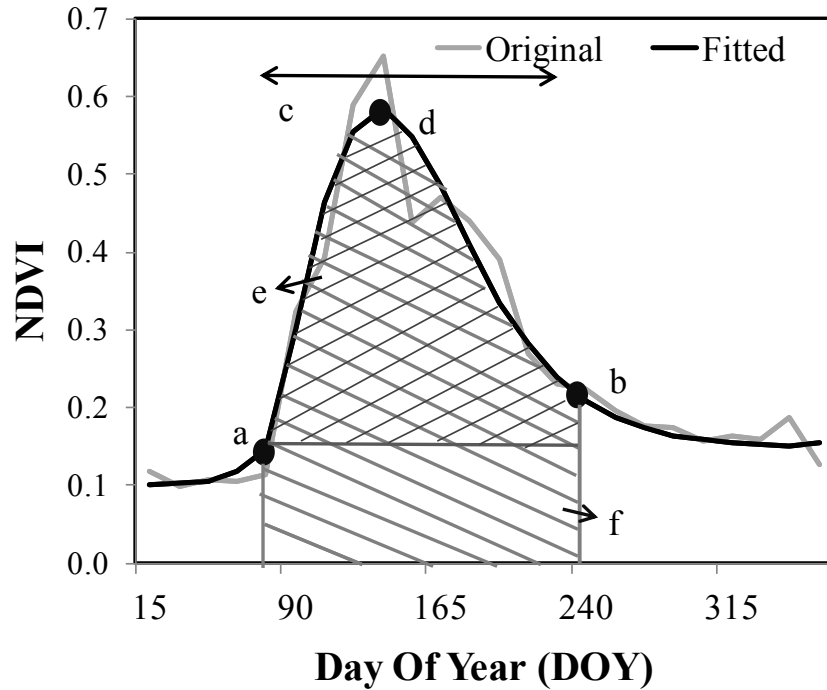


Figure 3-5. Phenological variables extracted

- a) Start of the growing season (SGS) is the time when the NDVI has increased to 20% measured from the left minimum.
- b) End of the growing season (EGS) is the time when the NDVI value has decreased to 20% measured from the right minimum.
- c) Length of the growing season (LGS) is the time from the start and the end of the season.
- d) Largest data value (NDVI_Peak) is peak NDVI value in the growing season.
- e) Small season integral (Sintegral) is the area between the fitted function and average line of left and right minimum.
- f) Large seasonal integral (Lintegral) is integral over the growing season giving the area between the fitted function and zero level.

The TIMESAT program was used (Jönsson and Eklundh 2002, Jönsson and Eklundh 2004) to accomplish most tasks.

3.5 Spatial Variation Analysis

After phenological information is obtained for each pixel, maps over the study area were made for each phenological variable in ArcGIS. Visual interpretation was applied in order to understand the spatial patterns for phenology parameters.

3.6 Temporal Trend Analysis

The NDVI time-series spans from 1982 to 2006. To detect trends of phenological parameters through these 25 years, Mann-Kendall trend test was used instead of common Ordinary Least Squares Regression (OLS) approach. Reviews of phenological trend studies have shown that the trend was usually detected using OLS and the significance was often tested by the F-test or T-test (Defila and Clot 2001, Eklundh and Olsson 2003). Few studies have applied the Mann-Kendall trend test (Latifovic and Pouliot 2007). The Mann-Kendall test is commonly used for hydrological data to detect randomness against trend in climatic time series (Xu et al. 2007). Linear regression is a commonly used procedure and easy to apply. However, linear regression has limitations and assumptions. Regression requires normality of the error distribution as well as constant variance of the errors and the method is very sensitive to extreme values. In contrast, the Mann-Kendall test does not assume any particular distributional form.

For the cases that $n > 10$, the test statistic z of a particular pixel is estimated by using:

$$z = \begin{cases} \frac{S-1}{\sqrt{Var(S)}} & S > 0 \\ 0 & S = 0 \\ \frac{S+1}{\sqrt{Var(S)}} & S < 0 \end{cases} \quad (5)$$

where

$$S = \sum_{i=1}^{n-1} \sum_{j=i+1}^n \text{sgn}(x_i - x_j) \quad (6)$$

$$Var(S) = \frac{\left[n(n-1)(2n+5) - \sum_t t(t-1)(2t+5) \right]}{18} \quad (7)$$

and

$$\text{sgn}(x_i - x_j) = \begin{cases} 1 & x_i - x_j > 0 \\ 0 & x_i - x_j = 0 \\ -1 & x_i - x_j < 0 \end{cases} \quad (8)$$

Where x is the variable, n is the number of years, t is the extent of any given tie (length of consecutive equal values).

The two-sided hypothesis was chosen here, indicating the time-series is either increasing or decreasing. The null hypothesis, H_0 , meaning that there is no statistically significant trend is accepted if $|z| \leq z_{\alpha/2}$, where α is the level of significance. In this research, the α is defined as 0.05.

In addition to identifying whether a trend exists, it is also very important to determine the magnitude of a trend. The magnitude of the trend was computed using the Sen's slope approach

(Sen 1968). Sen's slope method defines the trend magnitude β as the median of all slopes for all the pairs in the whole data set (Hirsch et al. 1982):

$$\beta = \text{median}\left(\frac{x_j - x_i}{j - i}\right) \text{ where } 1 < i < j < n \quad (9)$$

n is sample size, or the number of observations in the dataset. For a dataset of n years, if there are no missing data, the number of all possible combinations will be $n(n - 1)/2$. Because it uses the median estimates, this method is not sensitive to outliers. A positive value of β indicates an 'upward trend', i.e. increasing with time, whereas a negative value of β indicates a 'downward trend', i.e. decreasing with time. The pattern which has a transition point somewhere along the way was not considered in this study because Man-Kendall test only test the significance of one way (positive or negative) trends and Sen's slope is only conducted on the pixels with significant trend.

3.7 Driver Analysis

After the investigation on the spatial pattern and temporal trend on a regional basis, a zoomed in analysis is very important and necessary in terms of figuring out the drivers behind the phenological changes. Two related factors are investigated being land cover and climate. Specifically, the land cover changes based on LANDSAT imageries are detected. And the climatic factor is checked through comparing rainfall statistics and phenological variables.

3.7.1 Land cover change

High spatial resolution LANDSAT imageries were used to detect land cover change. First, image geometric correction was performed using the Image Geometric Correction module of the ERDAS image processing software (Version 9.1). Finally these images are in the Universal

Transverse Mercator (UTM) projection and the WGS 84 datum, and with a pixel size of 30m x 30m. The result RMS (root mean square) error was less than 1 pixel. Radiometric and atmospheric correction (using dark object subtraction method) was also conducted using the ERDAS software. The Digital Number (DN) values were converted to surface reflectance which is more reasonable after reducing impacts from different satellite and atmospheric conditions. Three bands (Blue, Red, and NIR) were combined and applied in classification because it is a classic combination characterizing vegetation. The classification scheme is defined as below:

Table 3-1. Land cover types used in TM/ETM classification

<i>Land Cover Types</i>	<i>Description</i>
Woodland/ Shrubland	Woody cover is over 30%
Savanna	Grassland with woody cover less than 30%
Cropland	Farmland used for agriculture
Water	Water bodies
Built-up	Artificial buildings

A hybrid unsupervised- supervised approach was used here. At first, about 70 spectral sub-classes were defined under unsupervised classification using the maximum likelihood method. Then with the help of visual interpretation, the sub-classes were identified and aggregated to target land cover classes. If necessary, the unclear sub-classes would be re-classified and aggregated later.

For each site, two images at individual years will be classified. Then a multi-date post-classification comparison change detection algorithm was used to determine changes in land cover. The post-classification approach provides ‘from - to’ change information and the kind of landscape transformations that have occurred can be easily calculated and mapped.

3.7.2 *Climatic factor*

As to the climate aspect, much literature has shown that plants in East Africa are mainly affected by precipitation. Thus precipitation is taken as the main climatic factor and analyzed with the phenological pattern. There are three kinds of precipitation characteristics that were computed in this study. One is the rainfall before the start of growing season which is very important to the germinating of plants because plants usually start growing after rainfall accumulates to certain amount. The next two are calculated using TIMESAT software. Time series of monthly rainfall data are processed by TIMESAT similar to the NDVI time series. The length and large integral variables were used in the analysis.

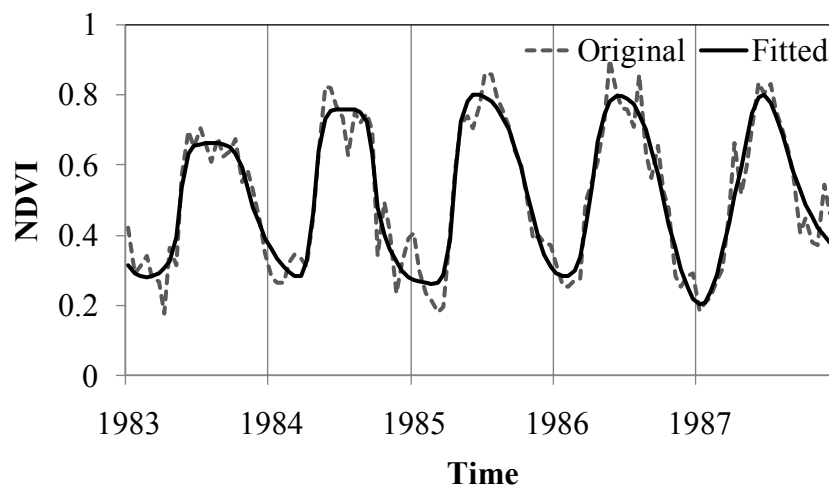
Chapter 4 RESULTS

4.1 Regional Phenological Attributes

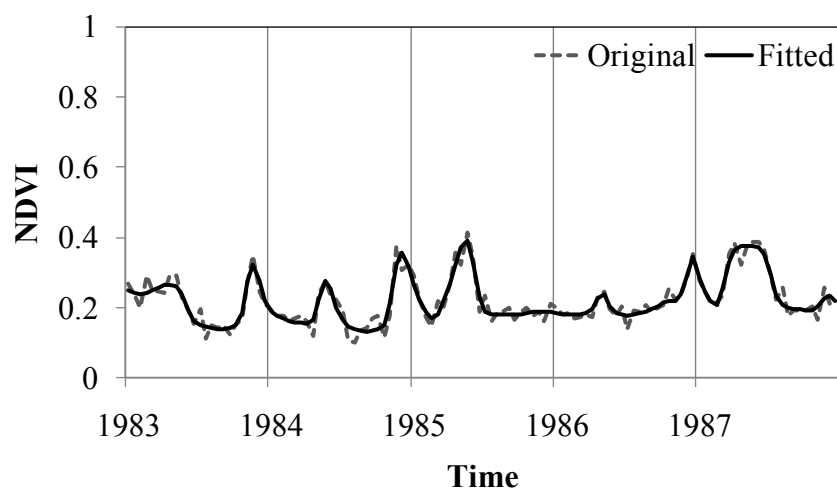
At first, phenological characteristic of different land cover types are displayed in section 4.1.1. Then the spatial patterns of each phenological parameter are shown in section 4.1.2. The section 4.1.3 explains how phenological parameter has changed at each pixel from 1982 to 2006 as well as the temporal shifts for the study area. In section 4.1.4, changes in annual rainfall and land use/cover is presented to help understand the drivers of observed phenological changes.

4.1.1 Phenological patterns for different land cover types

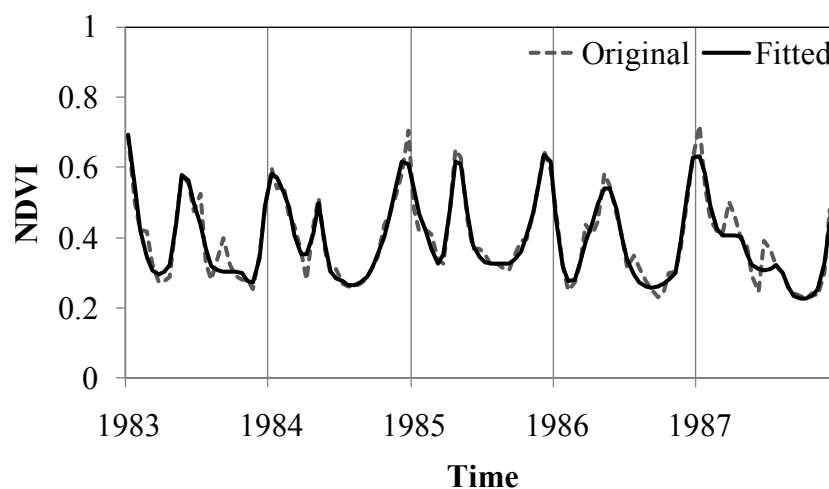
As described in the study area section (3.2), typical land cover types in East Africa are woodland and savanna. As ‘savanna’ is a general term, I refer to open grassland and wooded grassland in this thesis. They are different at species compositions and at different locations with unique climatic conditions. Thus it is important to observe the phenological patterns of typical land cover types. Five representative example pixels were selected and shown in the figure below.



a) A woodland pixel in northern Uganda

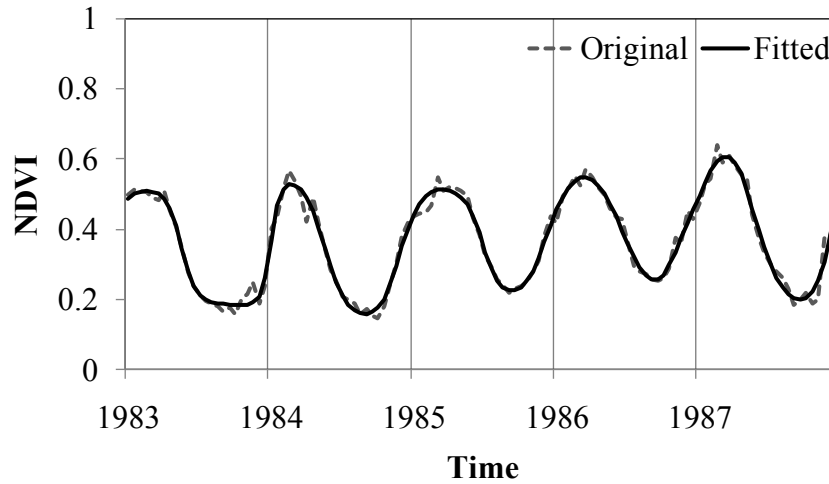


b) An open grassland pixel in northern Kenya

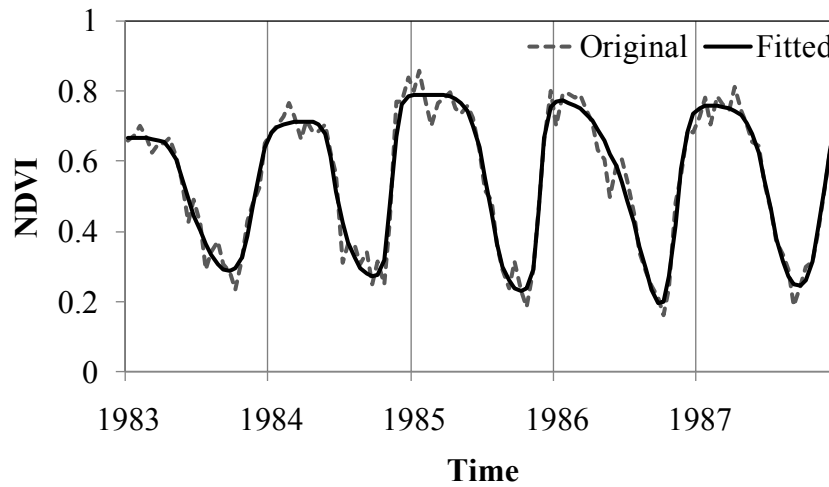


c) A wooded grassland pixel in south Kenya

Figure 4-1. NDVI profiles for typical land cover types in the study area



d) A wooded grassland pixel in central Tanzania



e) A woodland pixel in southern Tanzania

Figure 4-1 (cont'd)

Northern Uganda is mainly covered by forest and woodland. The NDVI curve of type a) in Figure 4-1 clearly shows that it is unimodal which means there is one distinct growing season in one year. Generally, the growing season starts near March/April and ends around November. The peak of NDVI is high which is around 0.8. One thing to be aware is that these values may be different between different pixels in this area. Even for the same pixel, the value can be different from year to year due to different climatic situations.

The 4-1.b and 4-1.c are in Kenya which is mainly covered by grasslands. They are both bi-modal plants which have two growing seasons in one year. There are general two seasons: one is in the first half of the year spanning from March/April to June/July; another is in the second half of the year spanning from October / November to January/February of next year. As to the amplitude of NDVI value, pixels in northern Kenya are lower than in southern Kenya which is determined by the land cover types. As shown in the figure 4-1, there are variations of NDVI profile between years. The timings, length, and amplitude of growing season are all different. Sometimes, the growing season even disappears because of the failure of rainfall.

The 4-1.d and 4-1.e are both in Tanzania. Different from the previous types, d) and e) starts growing season near the end of previous year (October - November) and the growing season continues into the next year (July - August). The 4-1.d and 4-1.e look very similar except that the NDVI amplitude of 4-1.e is higher than 4-1.d. The reason is that 4-1.d is representing wooded grassland or cropland pixels while 4-1.e is representing a woodland pixel.

In conclusion, three phenological types were found in this study. One is the bimodal pixels in Kenya, southern Tanzania, and southern Uganda, where vegetation has two growing seasons in one year. To be clear, the 'year' here does not need to be a calendar year because the growth of many plants can be interannual. The second is the unimodal pixels in northern Uganda where vegetation only has one growing season and starts growing in the early half of the year. The third is unimodal pixels in southern study area which starts growing near the end of the year or very early of the next year.

4.1.2 Spatial variations of phenological variables

After phenological parameters were extracted for individual years, the mean values of 25 years for each pixel were calculated and then mapped in order to present the spatial variations of those phenological characteristics over the whole study area.

Both unimodal and bimodal pixels exist in the study area and the growth periods are diverse. In this research, the phenological values were calculated on an interannual basis, e.g. July, 1982 to August, 1983. Thus the results presented as 1983 means the period July, 1982 to August, 1983. Season 1 indicates growing period in second half of 1982 for bimodal pixels and growing period through 1982 to 1983 for unimodal pixels (some start growing at early 1983 while some start growing at late 1982). Season 2 is only for bimodal pixels, e.g. growing period in the early half of 1983.

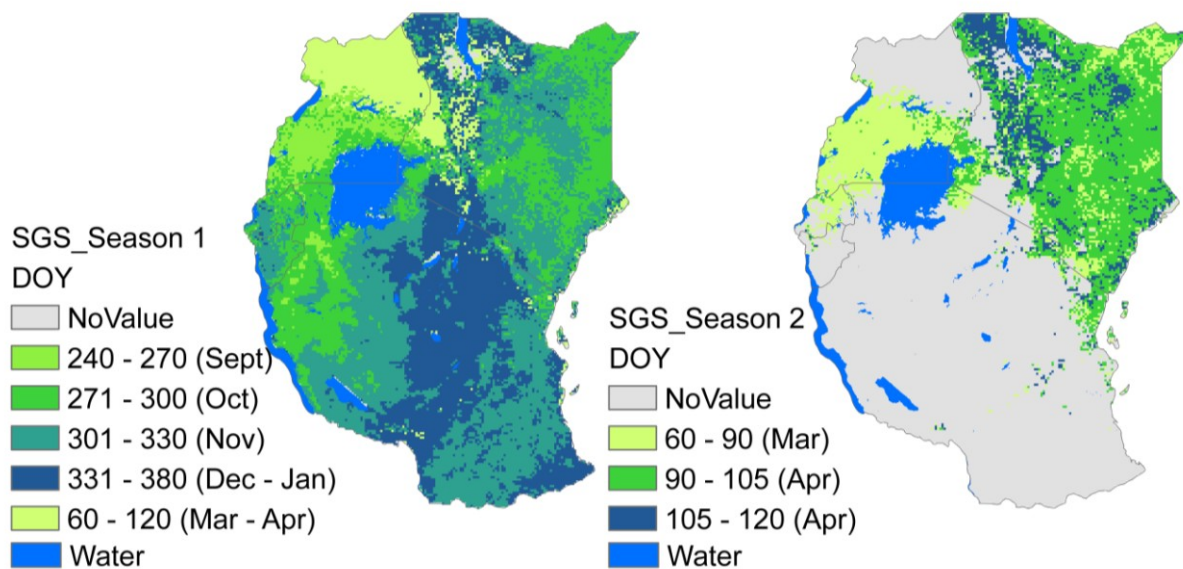


Figure 4-2. Spatial pattern of the start of growing season (SGS): SGS of Season 1 (left), SGS of Season 2 (right)

Obvious spatial variations of SGS could be observed from the figure 4-2. In northeast Ugandan, the SGS of the woodlands is mainly at the beginning of the year, centered on February

and March. The SGS of plants in southern part, like Tanzania, is near the end of the year, such as November and December. In Kenya and southern Uganda, the SGS of Season 1 is around September and October while the SGS of Season 2 is mainly in March and April.

The spatial trends of SGS are very obvious. In Season 1 map, there is a clear north -south trend: the SGS in northern part is earlier than in the southern part. Besides this north-south trend, there is a west-east tendency. Generally, the SGS is becoming later as the longitude increases. For instance, for Season 1, the SGS of west pixels is centered in late August and early September, while the SGS of east pixels is later into October. For Season 2, the eastern pixels are having a later start compared with pixels to the west. The SGS of those bimodal pixels around the Lake Victoria is in March. However, the SGS in Kenya is in early April.

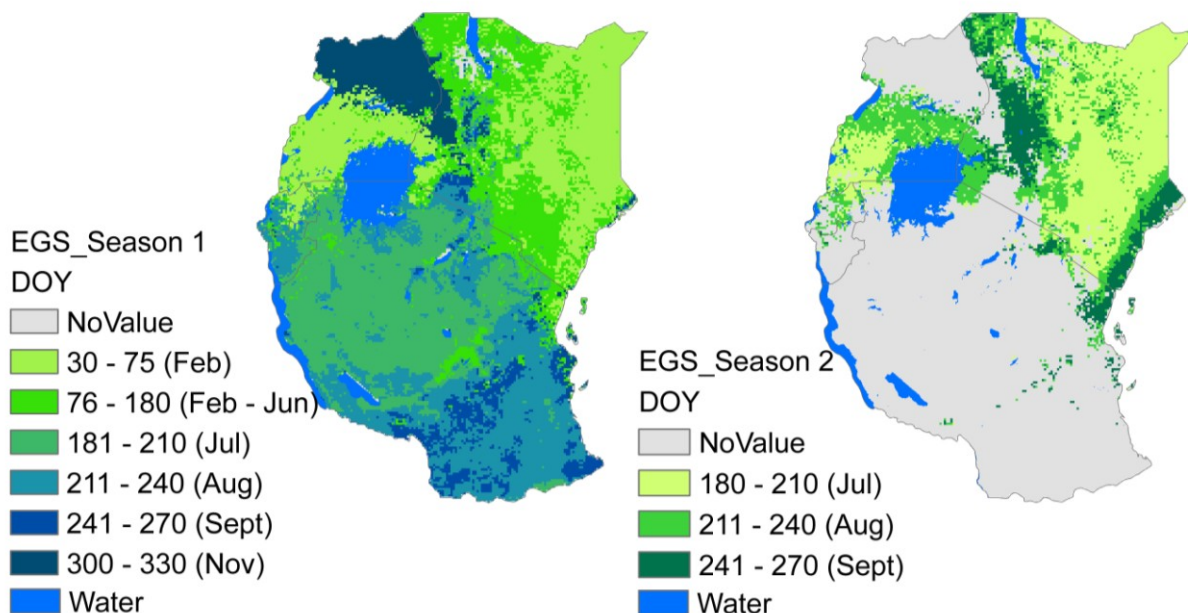


Figure 4-3. Spatial pattern of the end of growing season (EGS): EGS of Season 1 (left), EGS of Season 2 (right)

Similar with the SGS, the EGS is also showing a north -south trend. The pixels in Kenya are having the end in January and February. The pixels in northern Tanzania are ending the

growing season in June while the pixels in southern Tanzania are having the EGS around August. The EGS of pixels in northern Uganda is in November. The EGS of bimodal pixels in Kenya and southern Uganda are in July. The pixels at other areas, such as along the coast and surrounding the Lake Victoria, are having later EGS.

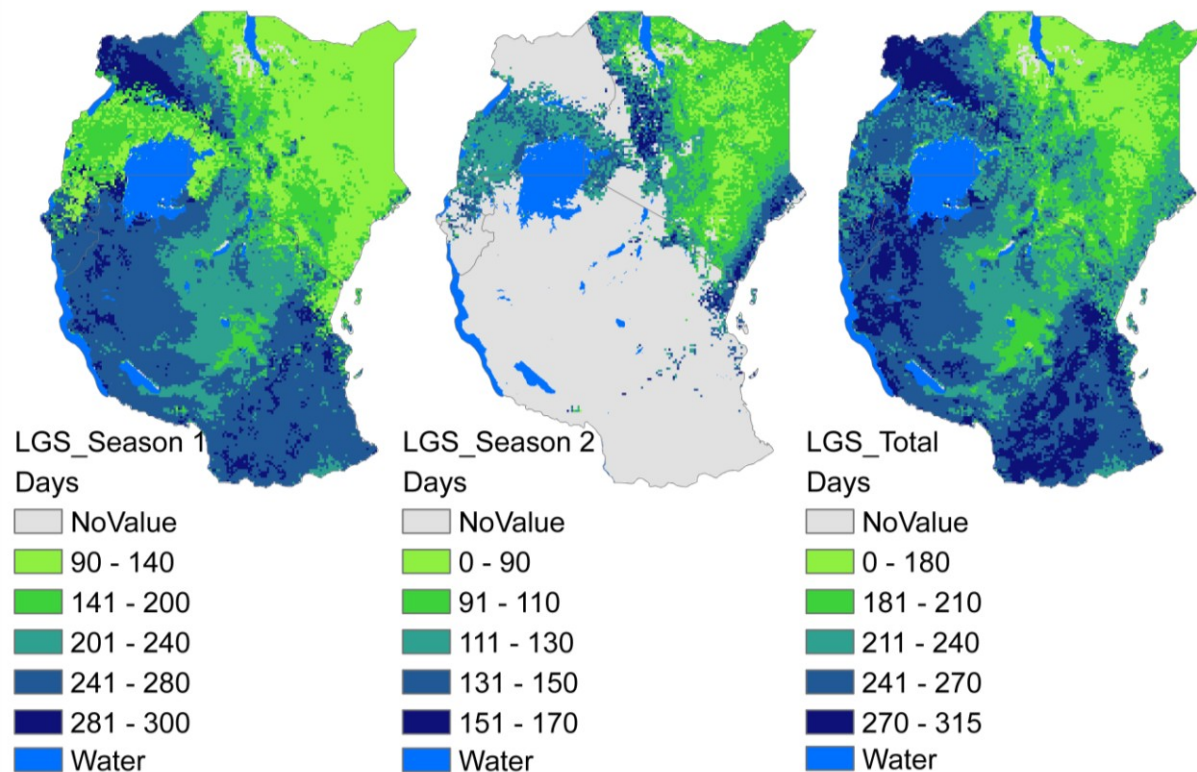


Figure 4-4. Spatial pattern of the length of growing season (LGS): LGS of Season 1 (left), LGS of Season 2 (middle), LGS of Season 1+ Season 2 (right)

Among unimodal pixels in north Uganda, the LGS of forest pixels is over 280 days while the LGS of woodland/shrubland pixels is shorter around 240 days. In central Tanzania, which is mainly covered by grassland and cropland, the LGS is around 201~240 days. In east and south Tanzania, which is covered by woodland, the LGS is approximately 241 ~ 280 days.

Among those bimodal pixels, most pixels in Kenya are having a LGS of 90 ~ 140 days for Season 1 and 90 ~ 110 days for Season 2. The pixels around the Lake Victoria are having a longer LGS of about 140 ~ 200 days for Season 1 and 110 ~ 130 days for Season 2. If the LGSs of Season 1 and 2 were added together, a LGS total map could also be made. North and central Kenya has a LGS around 180 days. Other places in Kenya are having a loner LGS, like coastal and highlands areas. Pixels around Lake Victoria are having a LGS about 240 days.

In general, the open grassland in north and central Kenya is having the least LGS. The wooded grassland in south Kenya and central Tanzania are having a longer LGS. The woodland pixels in north Uganda and west and south Tanzania are having the longest LGS. Despite of the locations, same land cover types tend to have similar LGS. For instance, the LGS of woodland in the north Uganda is very close to the LGS of woodland in Tanzania.

The north to south trend which exist in the SGS and EGS maps is not very clear here because the LGS is related with not only the rainfall but also the land cover types.

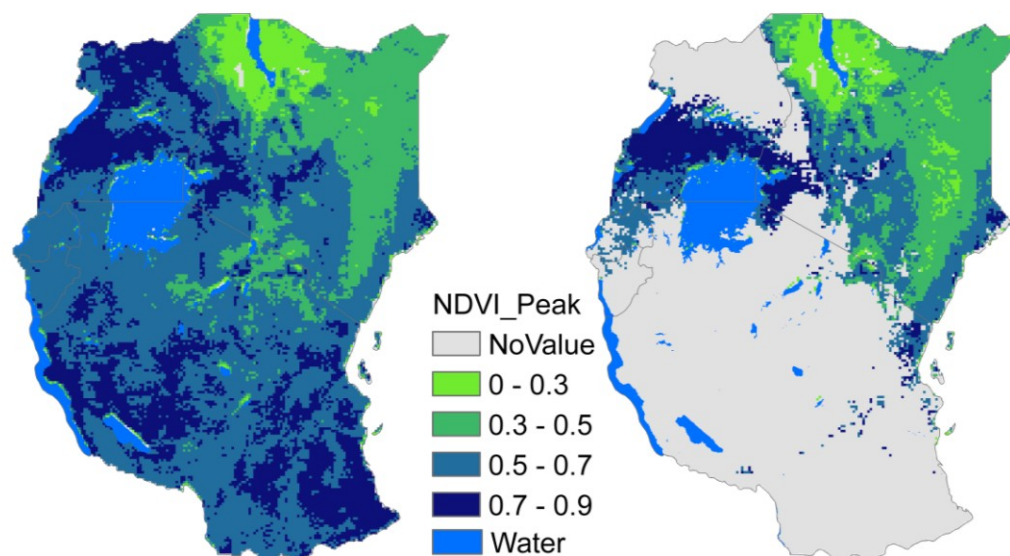


Figure 4-5. Spatial pattern of the NDVI_Peak of growing season: NDVI_Peak of Season 1 (left), NDVI_Peak of Season 2 (right)

NDVI_Peak is the largest NDVI value for the fitted function during the growing season. It is a good indicator of the vegetation growth amplitude. From figure 4-5, we can see that pixels in the northwest and south study area are having higher values compared with other pixels while pixels in north Kenya are having lowest peak values. In Season 2 map, the pixels around the Lake Victoria have much higher peak value than the pixels in Kenya. In Kenya itself, the north Kenya still have the lowest peak value. The east Kenya has a higher peak value than north Kenya. The coast and central area are having higher peak values.

Generally, the NDVI_Peak values of forest and woodlands are the highest. The wooded grassland and croplands are having lower peak values. The peaks of open grasslands in north and east Kenya are the lowest.

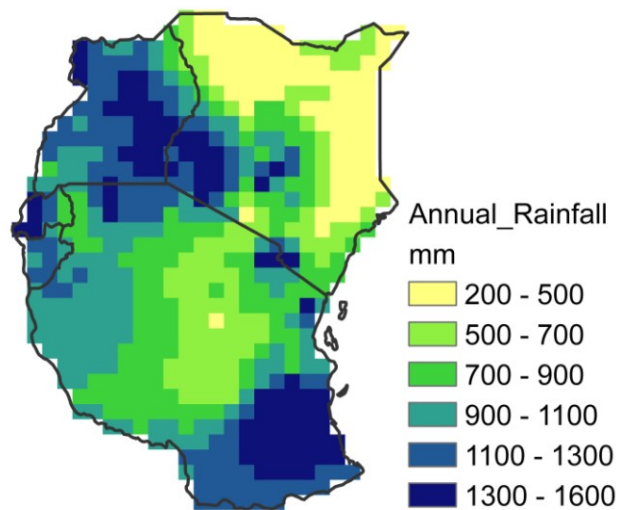


Figure 4-6. Spatial pattern of annual precipitation (Mean of 1982 -2006, CRU data)

To some extent, large integral (Lintegral) can be understood as proximity of annual biomass and Sintegral is taken as the annual net growth. The larger Lintegral value indicates more biomass production. The map shows that the area around Lake Turkana in northern Kenya has the lowest Lintegral. The southeast Kenya and northeast Tanzania has higher Lintegral but

south and northwest of the study area have the highest Lintegral. If the land cover is referred, we can see that sparse grasslands have least Lintegral. Lintegral of wooded grassland is higher but lower than the woodland which have the highest Lintegral.

The spatial distribution of Sintegral is very similar with the Lintegral except that pixels to the north of Lake Victoria are having smaller Sintegral while they have highest Lintegral. The reason is that the woodland, especially the forest, always has high biomass but the annual net productivity might not be that much.

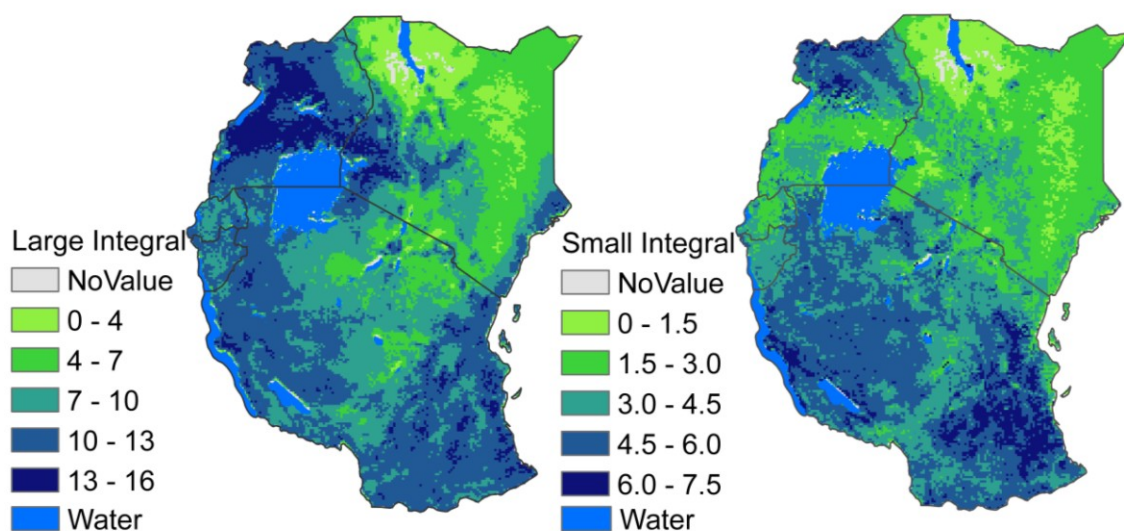


Figure 4-7. Spatial pattern of the large (left) and small (right) integral of growing season

In conclusion, phenological variables were spatially varied. Variables related with timings of growing seasons, such as SGS and EGS, are closely correlated with the rainfall patterns. The most important controlling factor is the movements of the Intertropical Convergence Zone (ITCZ), a band of low pressure where the trade winds of the northern and southern hemispheres converge. When the ITCZ moves towards north and south over the equator, it reaches a northernmost position in late July and a southernmost position in late January. The two rainy seasons in the equatorial latitudes are also produced by it: short rains of October to

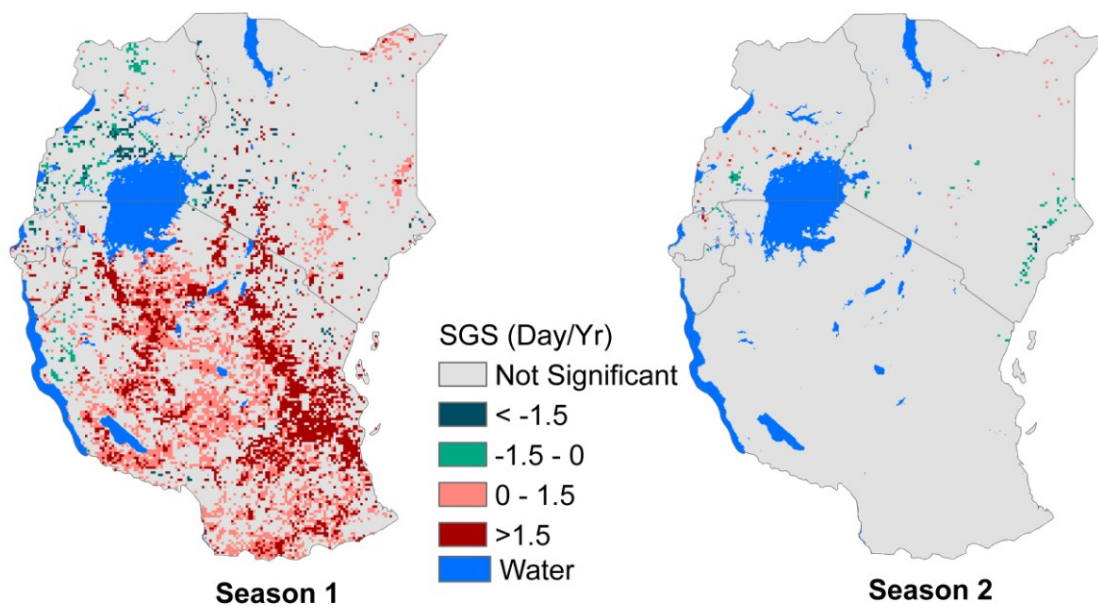
December and long rains of March to May occur when the ITCZ passes overhead. Actually, other factors, like the upper air jet streams, the Atlantic and Indian Oceans airs, and altitudes act along with ITCZ to affect the regional and local climate, which in turn control the timings of growing seasons. The spatial variation is also due to land cover differences because different land cover types tend to have different phenological patterns, even in similar climatic conditions. For instance, woodlands tend to have a longer growing season than the open grassland in nearby locations.

4.1.3 Phenological changes over time

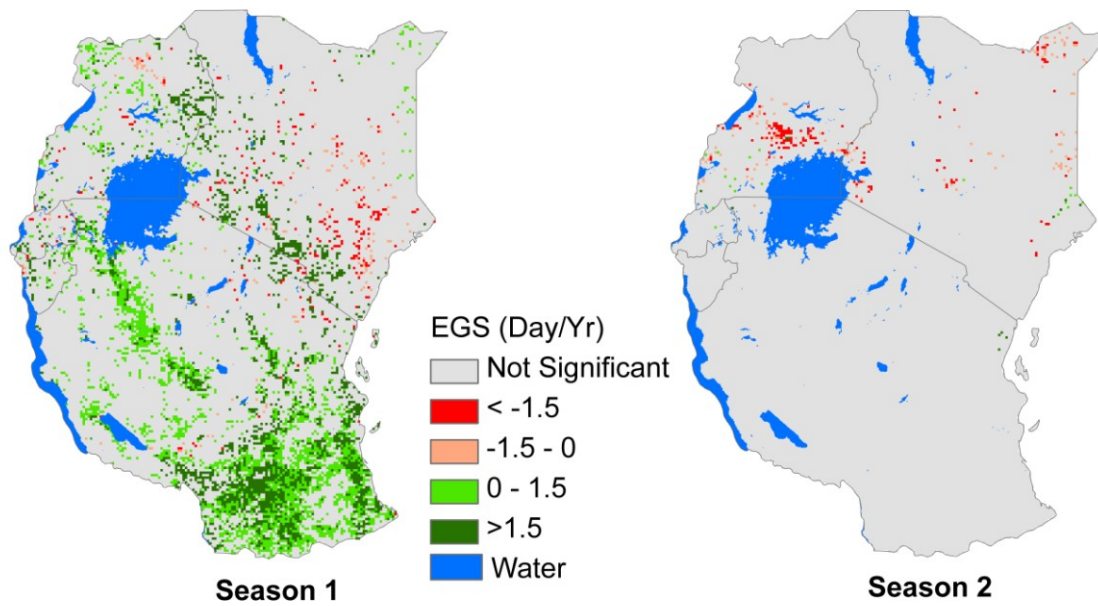
As global climate change is affecting the precipitation patterns in this region and land management strategies also change due to social-economic development, phenology of plants in this ecosystem may also have been impacted. This section will discuss how the phenological parameters have changed from 1982 to 2006 through trends analysis at the pixel level and histogram shifts over the whole study area.

4.1.3.1 Temporal trends at pixel level

Mann-Kendall test was used to identify significant trends at 90% confidence level and Sen's slope method was utilized to compute the magnitude of trends.

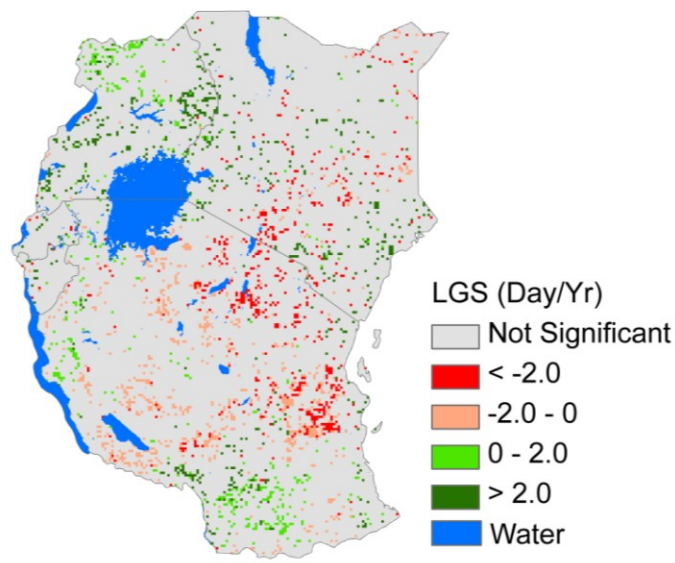


a) Trends of Start of Growing Season

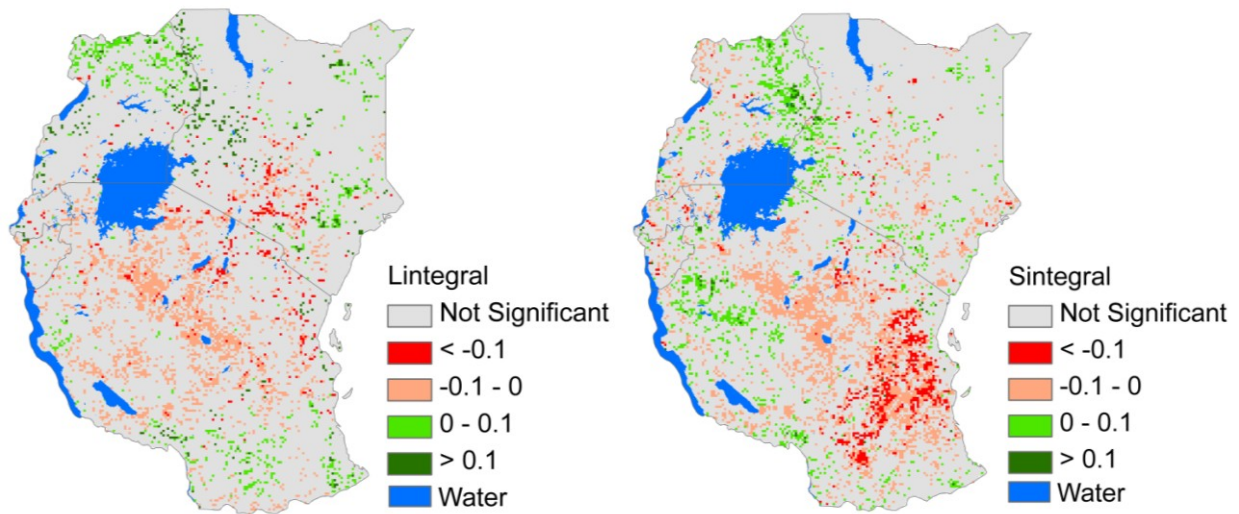


b) Trends of End of Growing Season

Figure 4-8. Maps of trends for phenological variables from 1982 to 2006: a, Start of Growing Season (SGS); b, End of Growing Season; c, Length of Growing Season; d, Large Integral; e, Small Integral



c) Trends of Length of Growing Season



d) Trends of Large Integral

e) Trends of Small Integral

Figure 4-8 (cont'd)

The results show that significant trends were discovered in many places in the study area. Positive and negative values refer to later and earlier dates for SGS and EGS. Significant positive trends of SGS, in other words, later SGS are widespread throughout the Tanzania and in some

places of southern Kenya. The SGS of most central Tanzania plants was delayed by about 1.5 day per year while the SGS in eastern parts was postponed more than 1.5 day per year. Some negative trends were found in central Uganda. The SGS has advanced around 1.5 day per year. Nevertheless, no significant trends were found at other locations. In season 2 map, there are no large patches of significant negative trends but some isolated and small patches along the coast of Kenya where SGS has advanced more than 1.5 day per year.

For EGS, large patches of positive trends were found in southern, central Tanzania, and southern, west Kenya, indicating that the EGS was delayed. The figure 4-8 shows that the EGS in central Tanzania was postponed less than 1.5 day per year while in southern Tanzania and Kenya the SGS was delayed a bit more. There are also some small patches of negative trends in southeast Kenya. In the season 2 map, several patches of negative trends occurred to the north of Lake Victoria and in northeast Kenya.

As to the LGS, negative trends indicates shorter growing season while positive trends means longer growing season. Patches of negative pixels were in central, northern Tanzania, and southern Kenya. The LGS has been shrunk by around 2 day per year. Positive trends were also found. The LGS in southern Tanzania has increased by less than 2 days per year. The LGS in parts of Uganda and Kenya has increased more than 2 days per year.

The positive and negative trends refer to increased and decreased production for Sintegral and Lintegral. There are large patches of negative trends of Lintegral in central Tanzania and southern Kenya. Positive trends were found at southern Tanzania, northern Uganda, and western Kenya. For Sintegral, large patches of negative trends were in central and eastern Tanzania. The Sintegral in eastern Tanzania decreased the most. Some small patches of positive trends were found in northern Uganda and western Tanzania.

Generally, the directions and magnitudes of changes are all spatially varied. The plants in central Tanzania tend to have a later SGS while the EGS did not change significantly, thus the length and productivity have reduced. On the contrary, in southern Tanzania, the plants are having both later SGS and EGS. The LGS and Lintegral have increased but the Sintegral on the contrary decreased. In northern Uganda, the SGS did not have significant change while the EGS was postponed, and the LGS, Lintegral, and Sintegral have increased. There are no large patches of significant trends found in Kenya. The changes noticeable are in southern Kenya where the SGS and EGS seemed to be later, the LGS, Lintegral, Sintegral tend to be less.

4.1.3.2 Temporal shifts for whole study area

The above analysis is examining the changes through the whole 25 years. However, there might also be fluctuations during this period. Thus I separated the 25 years into three periods: 1982 - 1989, 1990 - 1999, and 2000- 2006. Mean values of each period were calculated. And histograms of whole study area were made for each period. If we plot three histograms together, difference could be observed from the histogram shifts.

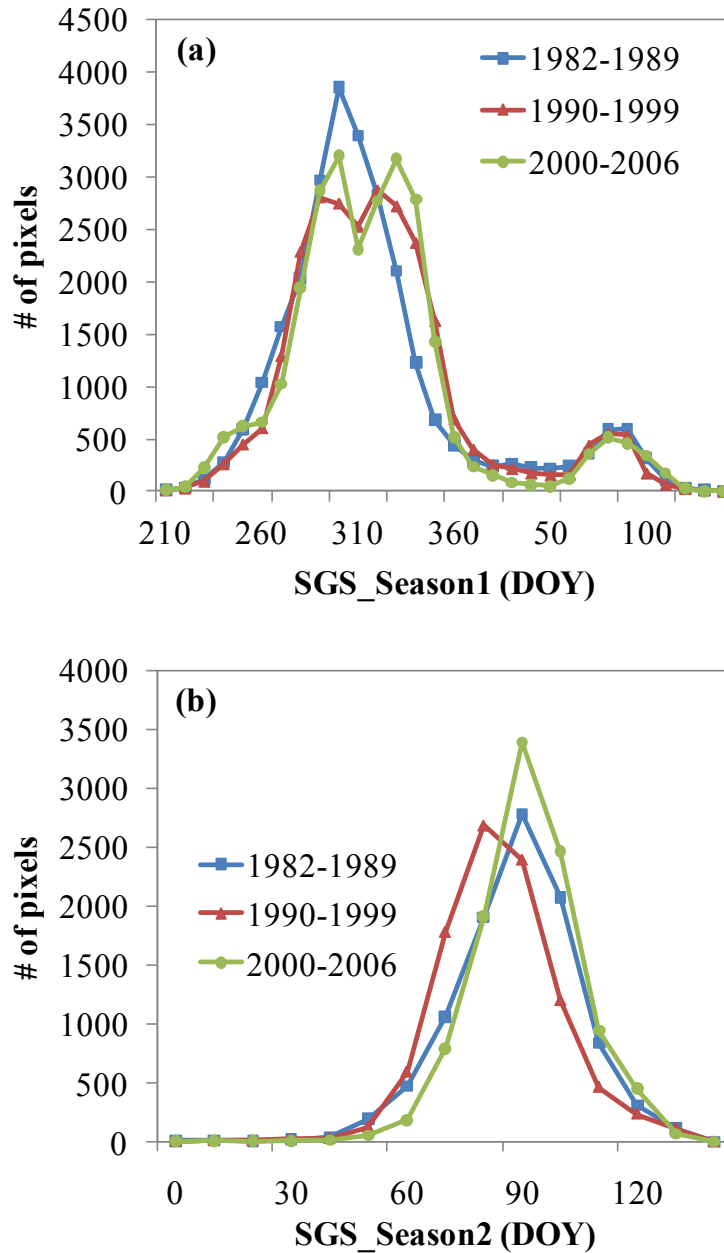


Figure 4-9. Histograms of whole study area for variable Start of Growing Season (SGS) shift between three time periods: 1982-1989, 1990-1999, 2000-2006. (a): Season 1; (b): Season 2.

There are two peaks of SGS_Season1 in the figure 4-9. One is around 300 DOY, and another is around 80 DOY. From the illustration of SGS in section 4.1.1, we know the season 1 of bimodal pixels and southern unimodal pixels start growing in the second half of the year so

that they compose the left half of the histogram. For northern unimodal pixels, they start the growing season in approximately March and thus compose the right half of the histogram.

The right part of the histogram did not change much during the three periods, meaning the SGS of southern unimodal pixels did not fluctuate much. But there were substantial shifts in the left part. Compared with 1980s (1982 - 1989), the histogram of 1990s (1990 - 1999) has shifted to the right which means that SGS has become later. And the histogram of 1990s also became wider which means that the variation among those pixels has increased. The histogram of 2000s (2000 - 2006) did not shift very much compared with 1990s but still shifted to right compared with 1980s. The width of histograms shows that the variations of SGS in the study area have been increasing.

The SGS of season 2 for bimodal pixels are also shown in the figure 4-9. Through the previous results, we know that the SGS will generally be in March and April. Peaks of three histograms are approximately in March. Compared with 1980s, the histogram of 1990s has shifted to the left which means the SGS has become earlier. In addition, the histogram of 1990s is the widest which means the variation is the largest. The histogram of 2000s has shifted to the right of 1990s and became similar with the 1980s which indicates that the SGS in 2000s has reverted to 1980s although the SGS was advanced in 1990s. In conclusion, the SGS of Season 2 has fluctuated between the three periods and had different direction of changes.

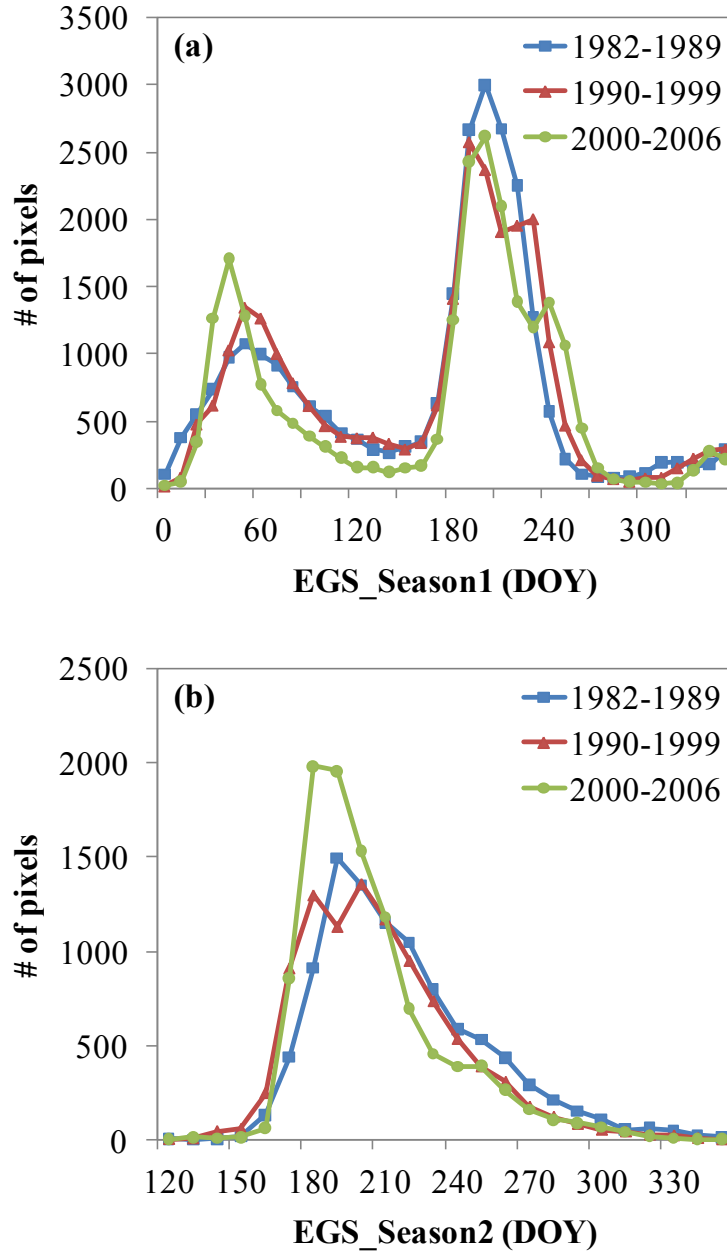


Figure 4-10. Histograms of whole study area for variable End of Growing Season (EGS) shift between three time periods: 1982-1989, 1990-1999, 2000-2006. (a): Season 1; (b): Season 2.

Similar with the SGS, there are also two peaks in the EGS season 1. One is around 60 DOY, and another is around 200 DOY. The season 1 for bimodal pixels usually ends in the early year which is the left part of the histogram curve. For the left part of the histogram, the 1990s has not shifted substantially compared with the 1980s, however the 2000s, especially the part to the

right of the peak has shifted to the left which means a lot pixels were having an earlier EGS. Both the northern and southern unimodal pixels ends the growing season near 210 DOY which composes the right part of the whole histogram. There were also substantial shifts in the right part. Compared with 1980s, the histogram of 1990s has shifted to the right which means the SGS has been later. In addition, the histogram of 1990s became widest indicating increasing variations. The histogram of 2000s continued to shift to the right and became wider. In conclusion, there was a continuous trend of later EGS for unimodal pixels while some bimodal pixels were having an earlier EGS.

The EGS of bimodal pixels in Season 2 showed that the histogram peak is around 190 DOY. Compared with 1980s, the histogram of 1990s has shifted to the left a little which indicates an earlier end of growing season. The histogram of 2000s continued to shift to the right and the width also shrank showing less variation. Generally, the EGS of season 2 tends to concentrate towards an earlier date.

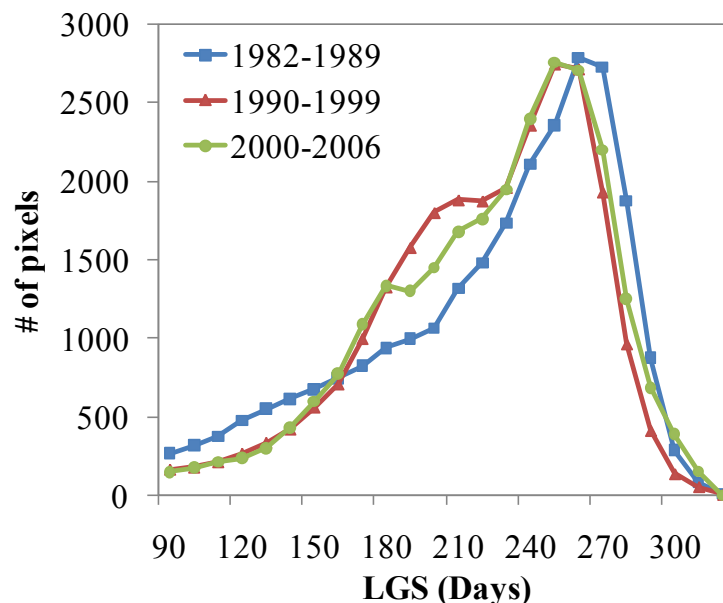


Figure 4-11. Histograms of whole study area for variable Length of Growing Season (LGS) shift between three time periods: 1982-1989, 1990-1999, 2000-2006.

The peaks of three histograms are all around 250 days. The section 1 ($LGS < 200$ days) more consist of open grassland pixels. The section 2 ($200 \text{ days} < LGS < 250 \text{ days}$) is more composed of those wooded grasslands and croplands. The last section ($LGS > 250$ days) is mainly woodland pixels. Compared with 1980s, the 1990s histogram has shifted to the left, indicating that the LGS has shrunk. The 2000s histogram has shifted to the right of 1990s a little. But both 1990s and 2000s histograms are to the left of 1980s which means that the LGS are generally becoming shorter.

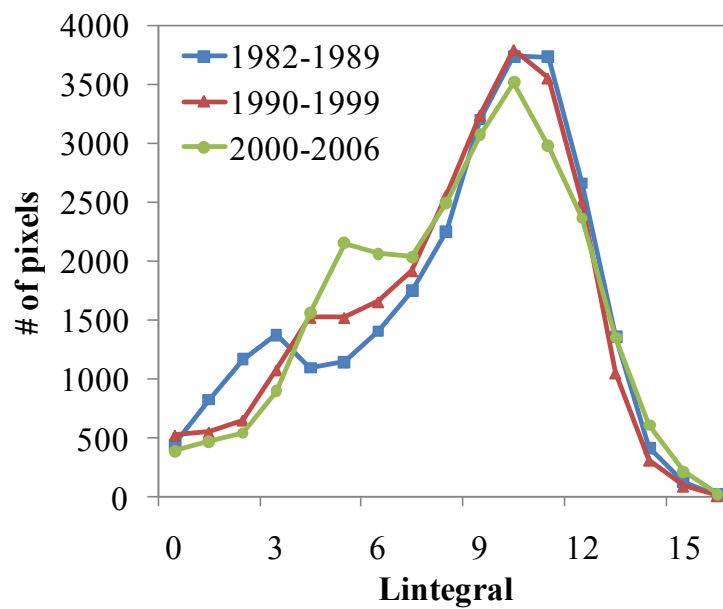


Figure 4-12. Histograms of whole study area for variable Large Integral of Growing Season (Lintegral) shift between three time periods: 1982-1989, 1990-1999, 2000-2006.

In figure 4-12, the part to the right of the peak (around 10) did not change much. But the left part has distinct changes. The 1990s and 2000s were both shifting to the left of the 1980s which means that the Lintegral has a tendency of decreasing.

This histogram analysis has revealed an interesting phenomenon, which was not detected by the trend analysis over 25 years. We found shifts for phenological variables between three

time periods indicating that phenological variables were going through many changes even though a one direction trend has not been observed.

4.1.4 Regional changes in land cover and annual precipitation

The above paragraphs have shown that phenology was changes. In order to understand the possible drivers of these changes, I looked at the changes in land use/cover and annual precipitation at the regional scale.

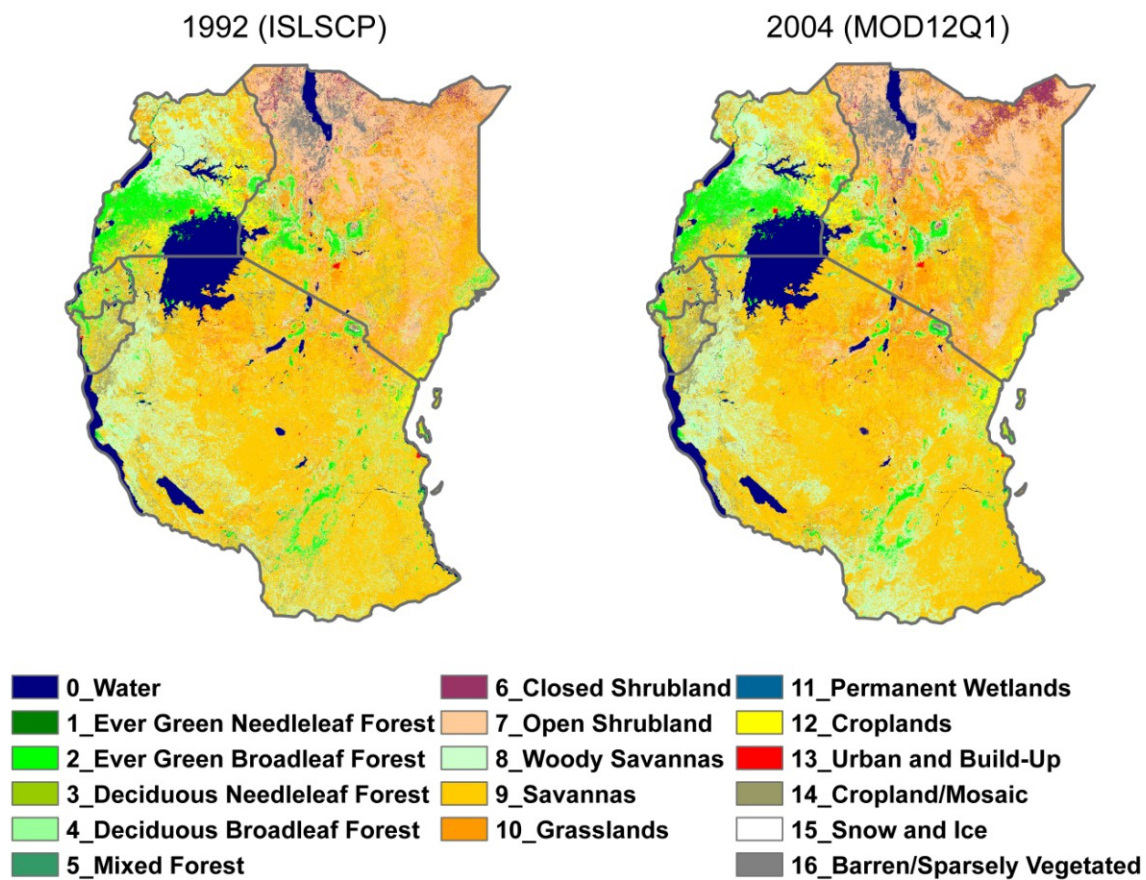


Figure 4-13. Land cover maps of East Africa: 1992 (IGBP DISCover); 2004 (MOD12Q1)

Table 4-1. Land use/cover change for East Africa (1992 - 2004)

<i>Land Cover Types</i>	<i>1992 (IGBP)</i>	<i>2004 (MOD12Q1)</i>
Water	6.23%	6.19%
Evergreen Needleleaf Forest	0.17%	0.08%
Evergreen Broadleaf Forest	4.51%	4.42%
Deciduous Needleleaf Forest	0.01%	0.00%
Deciduous Broadleaf Forest	0.48%	0.23%
Mixed Forest	0.19%	0.08%
Closed Shrublands	1.65%	1.71%
Open Shrublands	12.89%	12.21%
Woody Savannah	17.58%	16.89%
Savannah	38.64%	38.14%
Grasslands	8.93%	10.88%
Permanent Wetlands	0.15%	0.24%
Croplands	3.38%	3.49%
Urban and Built-Up	0.20%	0.20%
Cropland / Natural Veg Mix	3.04%	3.27%
Snow and Ice	0.00%	0.00%
Barren or Sparsely Vegetated	1.93%	1.95%

Figure 4-13 and table 4-1 above both indicated that land use/ cover were different from 1992 to 2004. Especially the statistics in the table showed decreases in forests, shrublands, and savannas, but increases in the croplands and grasslands. These kinds of change are highly due to the increasing human needs of agricultural lands which could result in clearance of natural forests, shrublands, and savannas.

Therefore we know the land use/cover is changing, what about the climate change? Thus how annual precipitation changed was also examined based upon CRU data. The figure 4-14 showed that there was only significant ($\alpha = 0.05$) decreasing trends for annual rainfall in the study area. These significant drying trends were mainly located in eastern Tanzania, north Uganda and Kenya. The changes in rainfall matched the changes in phenology to some extent.

For example, eastern Tanzania with decreasing annual precipitation was found to have significant decreasing trends for Lintegral and Sintegral (figure 4-8).

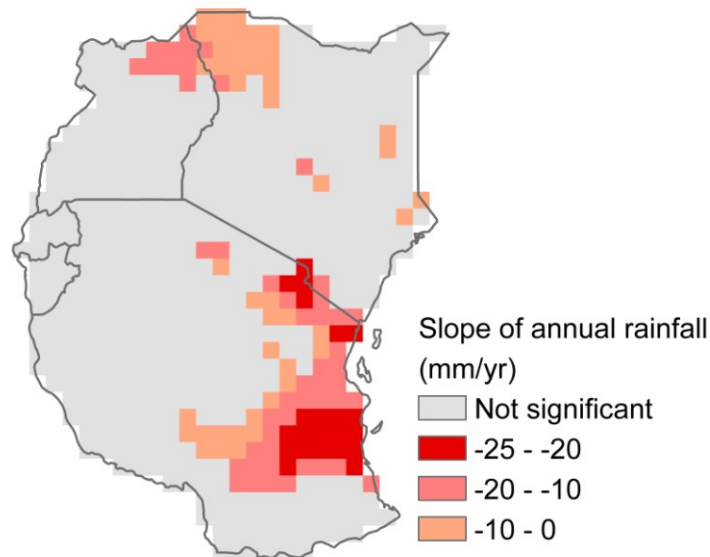


Figure 4-14. Map of trends for annual precipitation (CRU data: 1982 - 2006)

In conclusion, changes were observed at both land use/cover and climatic aspects at the regional scale. The two factors could both result in phenological changes. In order to get more precise information about drivers, I zoomed in to some hotspots and looked into the drivers of phenological changes at local scales.

4.2 Local Scale Understandings

The analysis above was focused on the whole study area. The overall characteristics were interesting because it helped to understand the spatial pattern of those phenological parameters as well as their changes. However, digging into several typical locations after getting the broad knowledge would be much meaningful. As we discussed before, phenology could change as climate and/or land cover changes. And, we also know rainfall pattern is the most important

climatic factor in this study area. Thus it is interesting to identify driving forces behind phenological changes by looking at both rainfall and land cover changes.

Based on the trend maps that we have (figure 4-8), two places with significant phenological changes were selected.

4.2.1 Tarangire National Park, Tanzania (Site I)

The first site is the Tarangire National Park (TNP) in Tanzania which is renowned for large populations of migratory mammals. It is fully protected and used only for wildlife tourism. It covers a large area of grasslands, wooded savanna, and flooded plains.

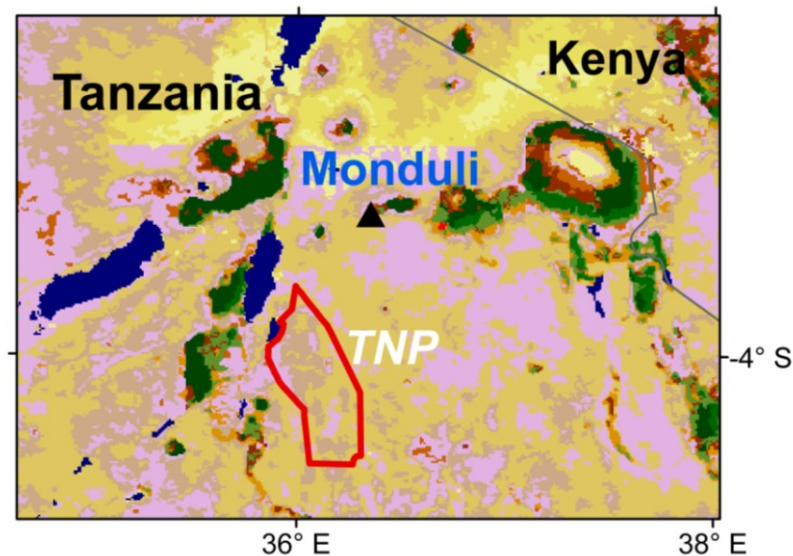


Figure 4-15. Location of site I

The area is characterized by a semi-arid climate. The temperature is stable all year long and varies only slightly around 22 - 27°C. There are distinct wet (October – May) and dry (June-September) seasons with high interannual oscillations and frequent droughts.

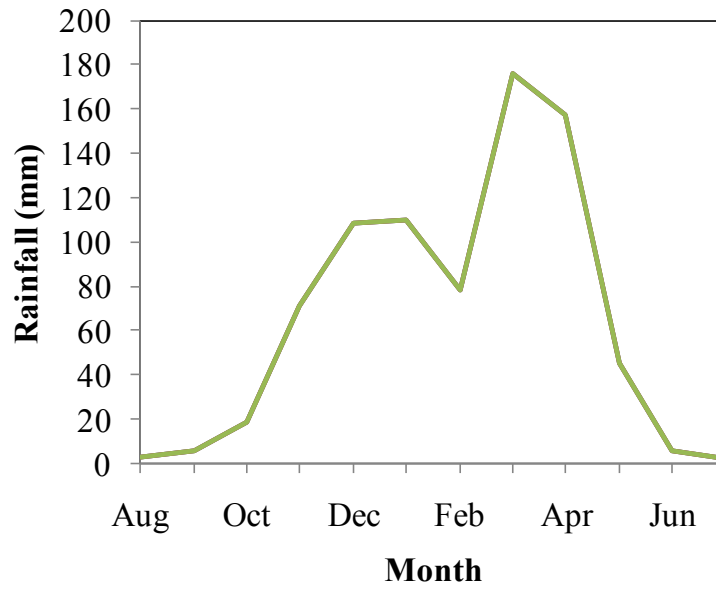


Figure 4-16. Mean monthly rainfall at Monduli station (-3.32°S, 36.35°E) from 1981 to 2008

According to the temporal trend maps above (Section 4.1.3.2.), the start, and end of growing season were delayed at this site, and the LGS, Sintegral, Lintegral all decreased.

As we know, the germinating of plants usually starts after rainfall accumulates to certain amount. The more that rain falls in the months before the start of growing season, the earlier the start date will be, and vice versa. Thus, our assumption is that the more abundant rainfall before the germination will result in an earlier start date, and consequently a smaller SGS value, and vice versa. In other words, the two should be negatively correlated. Therefore, I looked at the SGS and the rainfall before the SGS. As the SGS was about in November, the rainfall before SGS was calculated as the sum of rainfall from July to October. Monthly rainfall data was collected from station Monduli which is not far away from our area of interest.

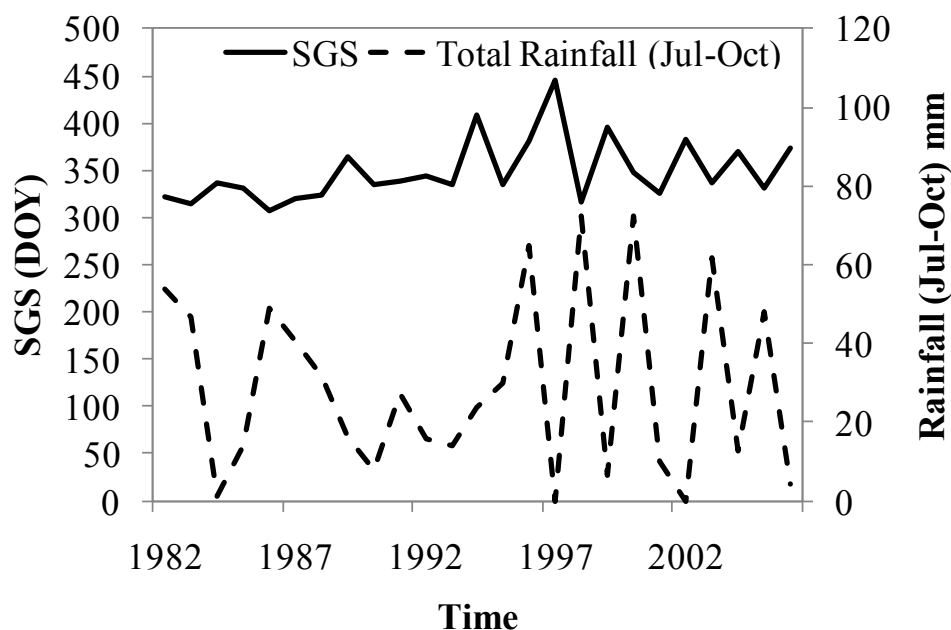


Figure 4-17. Comparison between SGS and Total rainfall before SGS at site I

In figure 4-17, the SGS is showing a substantial later trend however rainfall does not have a significant decreasing trend. But if we look at the increasing or decreasing bents in the SGS line, we would find that the corresponding bents in rainfall curve are in opposite directions. For instance, in 1996, the rainfall from July to October is very low. As a result, the SGS of 1997 was very late that year. The correlation coefficient between these two variables was calculated and turned out to be -0.44 which is not a very strong correlation but at least supports our assumption that the two are negatively correlated to some extent.

I am also interested at other phenological variables, such as LGS and Lintegral. Annual rainfall sounds like a good estimate but actually LGS and Lintegral are more dependent upon the distribution of rainfall other than the annual rainfall amount. Thus the monthly rainfall data was processed using TIMESAT in order to get useful precipitation characteristics which can be compared with the phenological attributes.

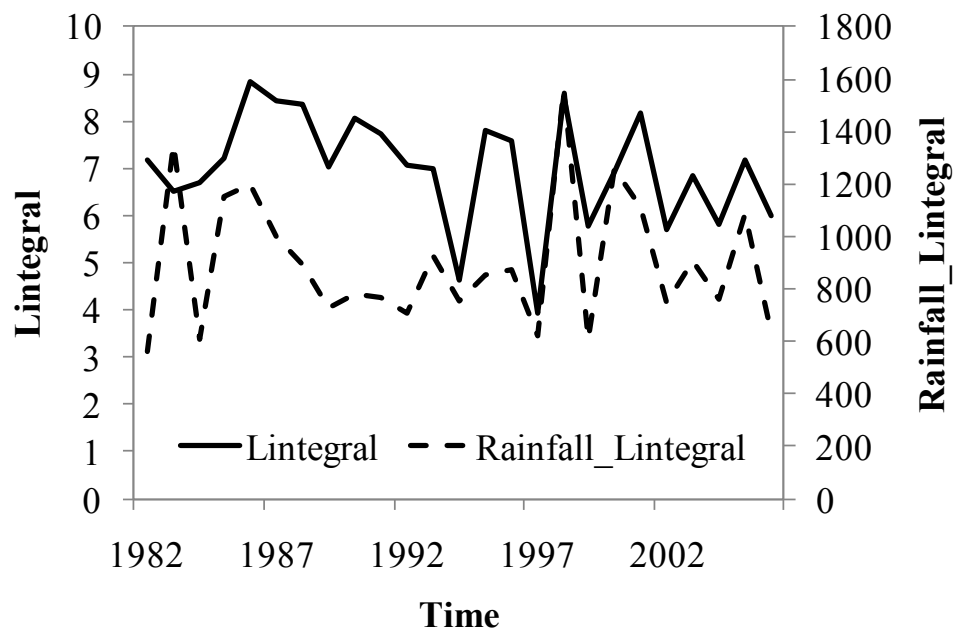
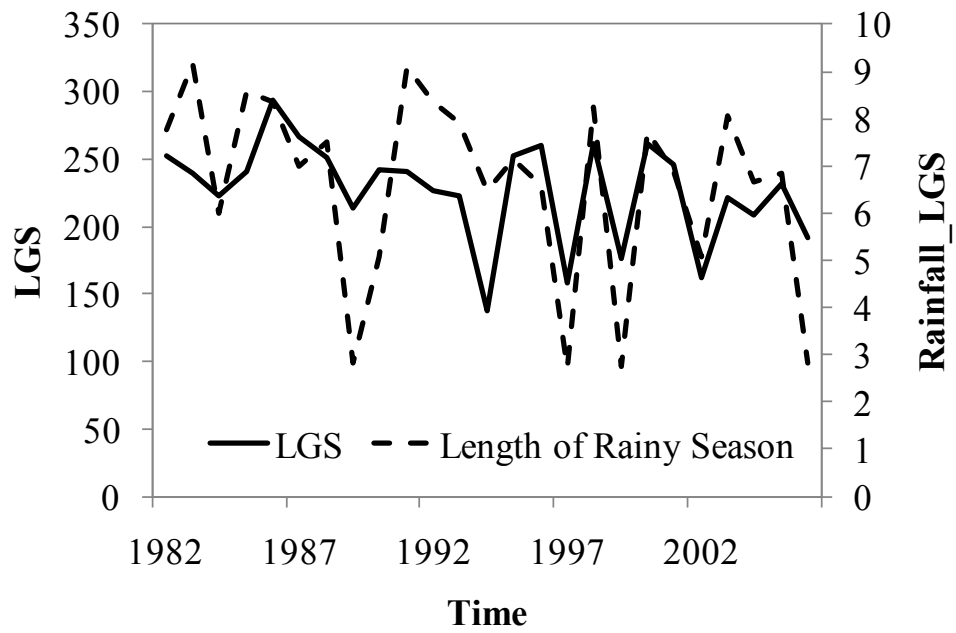


Figure 4-18. Comparison between the LGS and Rainfall_LGS; Lintegral and Rainfall_Lintegral at site I

The assumption here is that the LGS should be positively correlated with the length of rainy season (Rainfall_LGS). A longer LGS is corresponding to a longer Rainfall_LGS, and vice versa. Similarly, the Lintegral is also positively correlated with the large integral based on rainfall data (Rainfall_Lintegral). Figure 4-18 above shows that the LGS and Rainfall_LGS are well correlated: the two are showing very similar changes. The Lintegral and Rainfall_Lintegral are also showing similar trends. The correlation coefficient is 0.62 for LGS and Rainfall_LGS, and 0.50 for Lintegral and Rainfall_Lintegral. It proves the assumption that they are positively correlated and shows that rainfall is a main factor influencing the phenology here.

Results from fine resolution MODIS data were also employed here to better explain the phenological changes and extend the time period to year 2008.

Because the datasets from GIMMS and MODIS have many differences: different sensor, different spatial resolution, different vegetation index, etc, the difference between the phenological values are not discussed here. Firstly, we can tell that results from the GIMMS and MODIS in 2000 – 2008 are showing very similar changing patterns. Thus I am very confident that this fluctuation in recent decade is not errors from the data or process but determined by other factors. Another phenomenon to be noticed is that for all three phenological parameters, they are showing very significant trends from 1982 to 1994, for instance, the SGS is increasing while LGS and Lintegral are decreasing. However, after 1994, obvious trends have gone, instead, these phenological variables began to fluctuate substantially between years. Similar changes were also shown in rainfall characteristics. In conclusion, I believe that at this site, the phenological changes are mainly due to the changes in precipitation patterns. However, this conclusion is too early to be made until the influences from land cover changes have been eliminated.

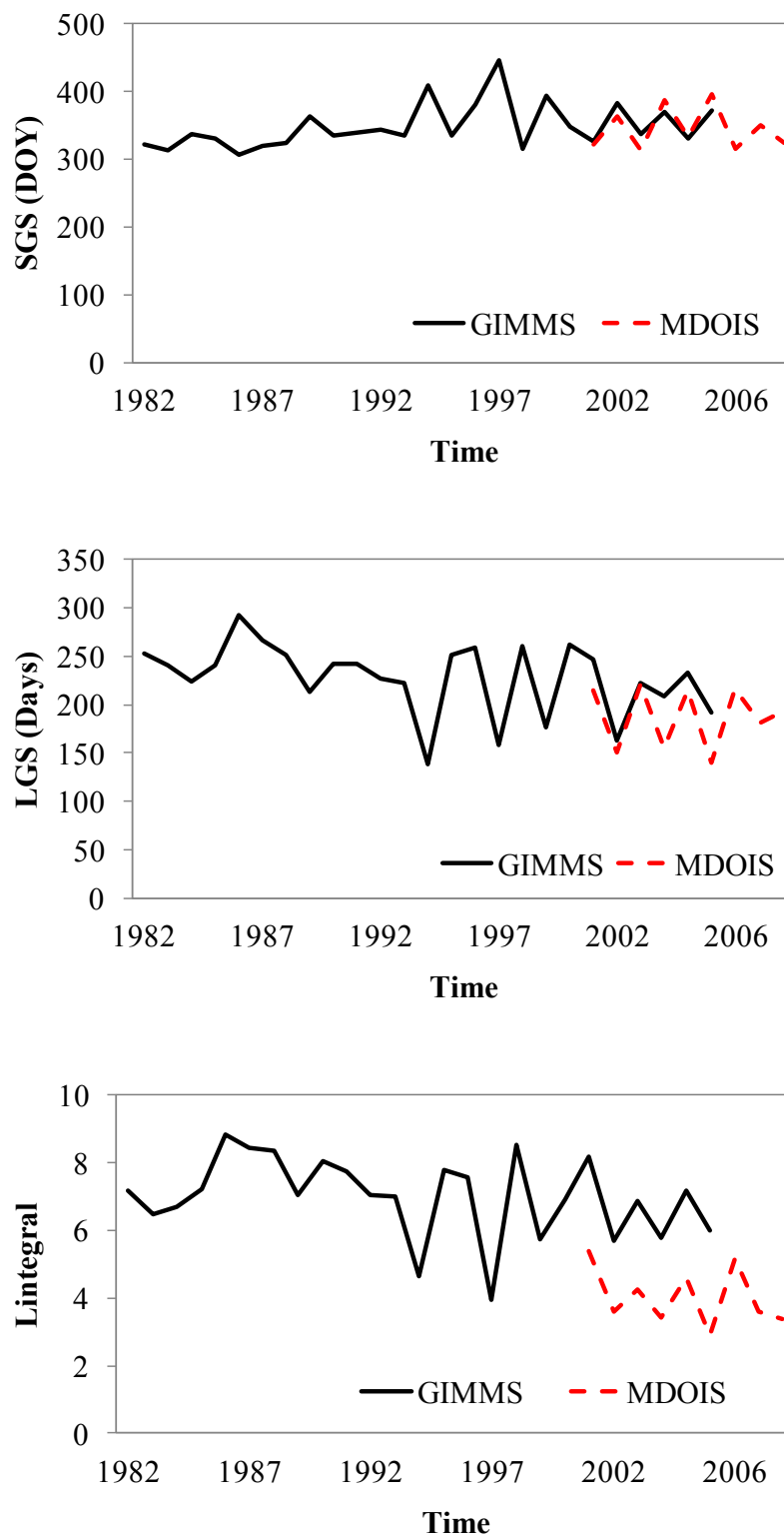


Figure 4-19. Results from GIMMS data against results from MODIS data

Hence, the next step is to check the land cover changes. Two Landsat images at Path 168 and Row 063 at different dates were selected. One is on January 18, 1985 and another is on February 21, 2000. January and February is in the rainy season for this area thus it is a good time to detect vegetation. And the two images were temporally close in order to minimize the influence from phenology. Land cover classification was done on each map separately and then the land cover changes were listed.

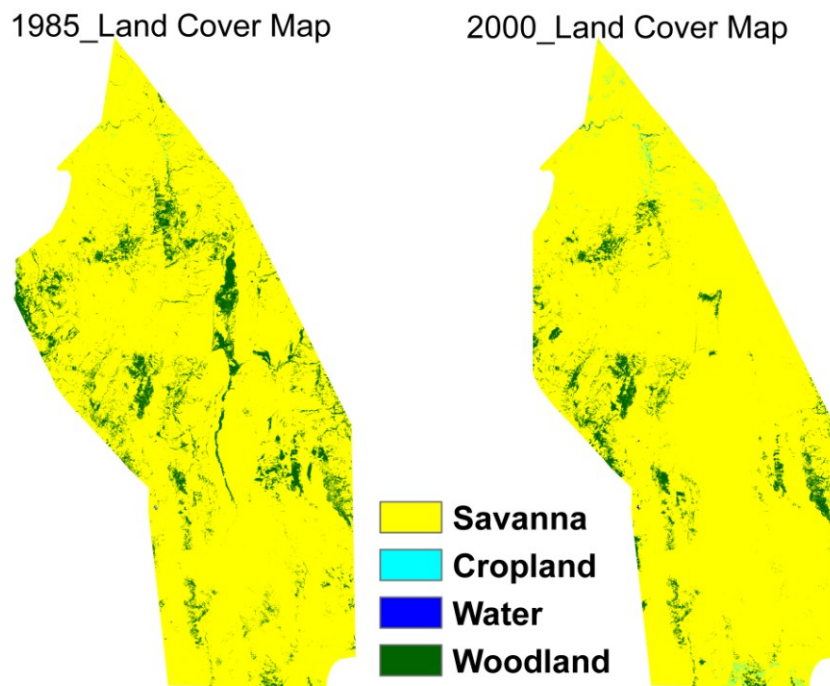


Figure 4-20. Land cover classification maps (based on Landsat images) of site I in January, 1985 and February, 2000

This area is covered by savanna and woodlands. One obvious change is that the woodland is disappearing along the Tarangire River. This is highly due to the different rainfall conditions between 1985 and 2000. Compared with that of 1985, the rainfall is much less in year

2000 which may have resulted in the late growing of woodland in 2000. Other than that, there were no substantial changes. In addition, the change detection statistics was calculated.

Table 4-2. Land cover change matrix for site I (1985 - 2000)

<i>2000</i> <i>1985</i>	<i>savanna</i>	<i>cropland</i>	<i>water</i>	<i>woodland</i>	<i>Total</i>
savanna	90.23%	0.28%	0.01%	0.93%	91.45%
cropland	0.00%	0.04%	0.01%	0.00%	0.05%
water	0.01%	0.00%	0.00%	0.00%	0.01%
woodland	3.85%	0.01%	0.00%	4.62%	8.48%
Total	94.09%	0.33%	0.02%	5.56%	100.00%

The cropland did not change much because the TNP is under protection from human activities. The percentage of savanna increased while the percentage of woodland decreased as some woodland was converted into savanna. The amount of change is not substantial and the savanna could still contain woody covers, therefore, land cover is not thought to change a lot here. Thus land cover change is not taken as a major influencing factor for this site.

To sum up, the comparison between the rainfall statistics and the phenological variables shows close correlation. On the other hand, there are not substantial amounts of land cover changes so the influences from land cover changes can be eliminated. Thus, at this site, changes in rainfall patterns were accounting for most changes in the phenological variables.

4.2.2 Tabora District, Tanzania (Site II)

The second site is chosen in central Tanzania, ranging from longitude 33 ° E ~ 33.5 ° E and latitude 4 ° S ~ 4.5 ° S.

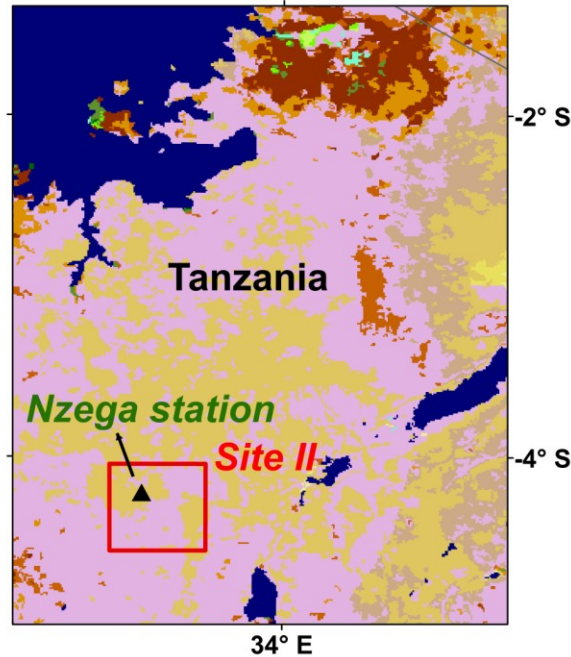


Figure 4-21. Location of site II

According to the temporal trend maps above (Section 4.1.3.2.), the SGS tends to be later from 1982 to 2005 at this site. The Lintegral and LGS were decreasing. Similar with what was done in section 4.2.1, the first step is to investigate the relationship between the SGS and rainfall before SGS. The assumption here is also that the SGS and the rainfall before SGS have a positive correlation. At this site, the SGS is also around October. So the rainfall before SGS is the sum of rainfall from July to October. Monthly rainfall data were from a station called Nzega (4.21°S, 33.18°E) and CRU TS 3.1 data.

In figure 4-22, the SGS is showing an increasing trend. Rainfall fluctuated but showed an insignificant slightly decreasing tendency. Generally, the changing direction of SGS is on the opposite of the rainfall before SGS visually. And the correlation coefficient was calculated to be -0.30. This proved our assumption that these two variables were negatively correlated, but the correlation is not very strong.

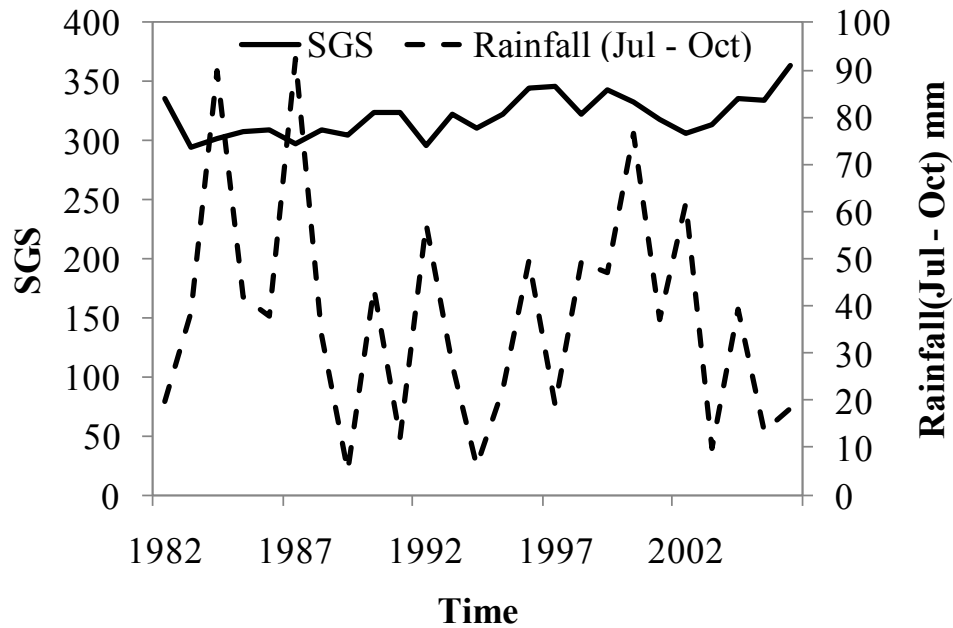


Figure 4-22. Comparison between SGS and Total rainfall before SGS at site II

LGS and Lintegral were then also compared with rainfall parameters computed through TIMESAT.

Similar with the previous site, I assume that higher Rainfall_LGS and Rainfall_Lintegral will result in higher LGS and Lintegral respectively, which means that two variables should be positively correlated. In figure 4-23, the LGS is showing a decreasing trend while there were no significant negative trends existing in Rainfall_LGS. Visually, the changes of two are in the same direction but not very closely related. The Lintegral was also showing a decreasing trend and Rainfall_Lintegral also showed a negative trend. It seems that the trends of these two parameters were matching. Then the correlation coefficients were calculated. The correlation between Lintegral and Rainfall_Lintegral is 0.36 which indicates a positive correlation. But surprisingly, it is -0.04 between LGS and Rainfall_LGS which is a very weak negative correlation.

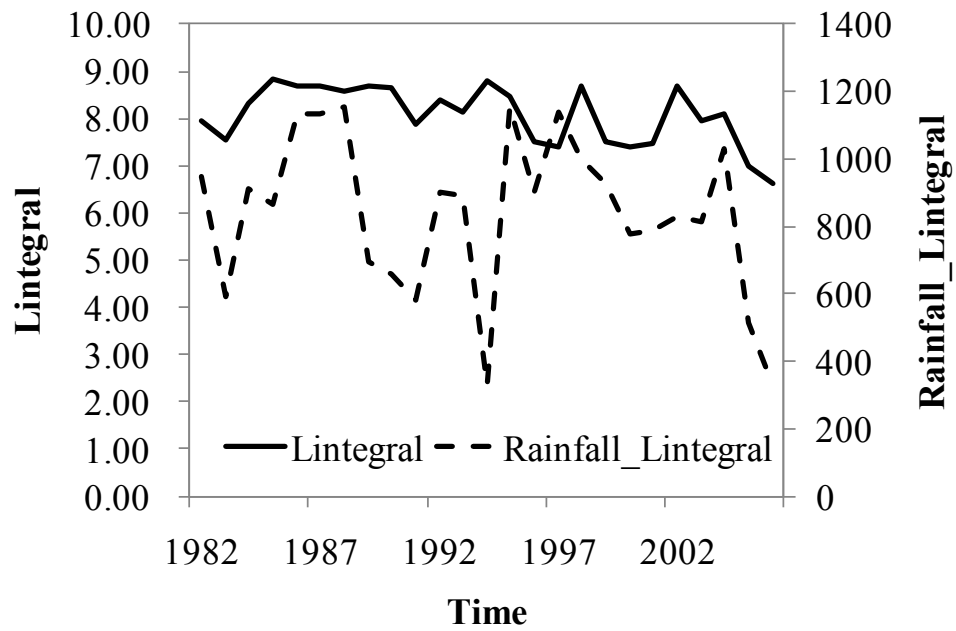
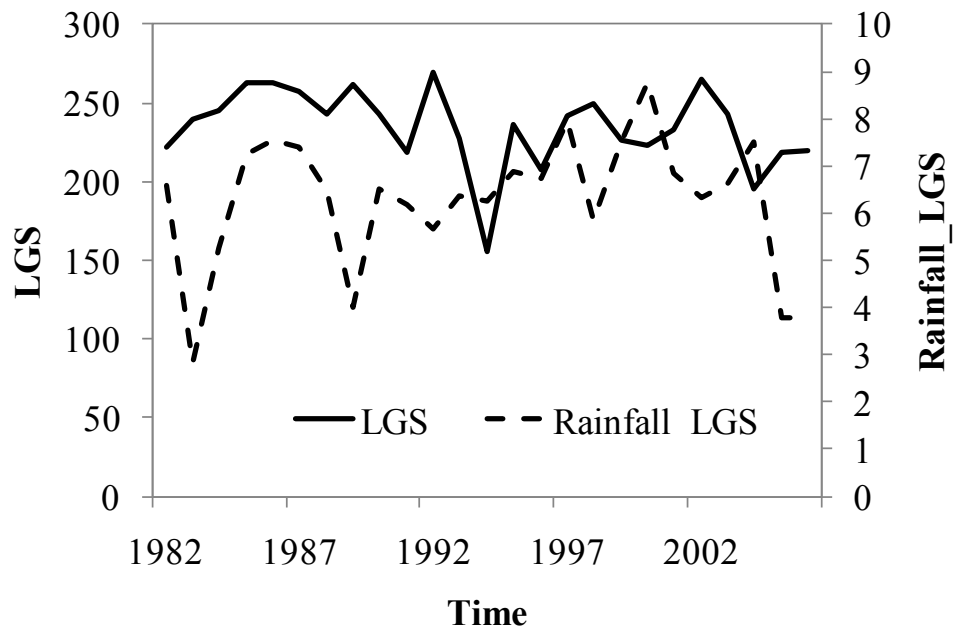


Figure 4-23. Comparison between the LGS and Rainfall_LGS; Lintegral and Rainfall_Lintegral at site II

It seems that rainfall cannot explain the variance in the phenology. There has to be other factor controlling the phenological changes. Is it possible that land cover changes were playing

an important role? Two Landsat images at different dates at Path 170 and Row 063 were selected. One is on March 5, 1985 and another is on May 18, 2003. The two images selected at close dates helped to minimize the influence from phenology. Land cover maps in 1985 and 2003 were produced.

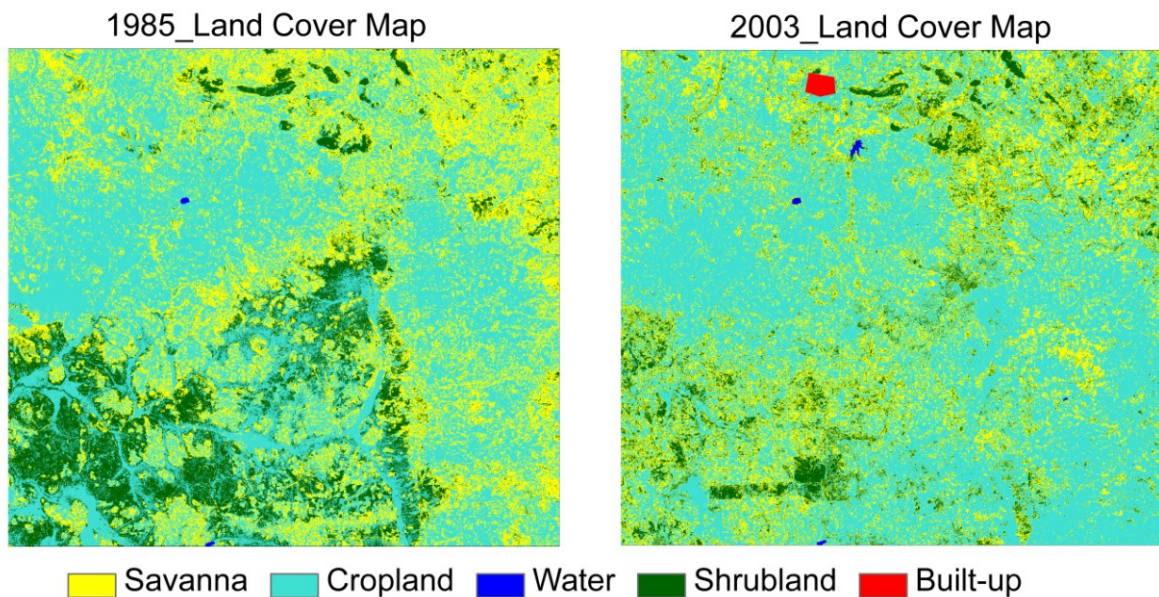


Figure 4-24. Land cover classification maps (based on Landsat images) of site II in March, 1985 and May, 2003

Table 4-3. Land cover change matrix for site II (1985 - 2003)						
2003 \ 1985	<i>savanna</i>	<i>cropland</i>	<i>water</i>	<i>shrubland</i>	<i>built</i>	<i>Total</i>
savanna	11.29%	16.48%	0.03%	2.53%	0.08%	30.41%
cropland	12.17%	41.76%	0.03%	2.27%	0.04%	56.27%
Water	0.00%	0.00%	0.03%	0.00%	0.00%	0.03%
shrubland	4.46%	5.42%	0.00%	3.33%	0.08%	13.29%
Total	27.92%	63.66%	0.08%	8.13%	0.21%	100.00%

The two maps show obvious shrubland degradation and increasing cropland. And the change detection statistics shows the same results. A large portion of shrubland was converted into cropland, and some savanna was also taken up by cropland. Since this site is largely covered

by cropland, this may help to explain the negative relationship between the LGS and the Rainfall_LGS. The croplands are highly affected by human management, which is very different from the natural savanna. The timings for seeding and harvesting are controlled more by human decisions other than the natural precipitation. Thus the precipitation changes did not show strong relationship with the phenological changes. In conclusion, this site was more influenced by the human activities, including land cover and cropland management changes.

Chapter 5 DISCUSSION and CONCLUSIONS

This research extracted phenological variables from time series of remotely sensed data. Remotely sensed data has provided an effective way of mapping, monitoring, and quantifying phenological changes, especially in places where ground observations are missing. Although the phenology information derived from remotely sensed data is only an approximation of the true plant biology because of spatial resolution issue, large spatial and temporal coverage make remotely sensed data a good choice to study phenology. The long term GIMMS NDVI dataset covers a 25 years period spanning from 1982 to 2006, which is very useful at studying phenological patterns at regional scales. On the other hand, the MODIS EVI dataset is available for a shorter period from 2000 to 2010 but with higher spatial resolution, which can be helpful at smaller scales. In summary, these datasets can meet the majority of needs in this study.

Various phenological variables derived from remotely sensed data helped to better understand the complicated phenological pattern. The phenological variables selected in this thesis focused on important properties of phenology, including the timing characteristics, the seasonal length and magnitude, and the production. These variables can reflect crucial aspects of phenological patterns and the changes.

Great variability exists in the phenology patterns over the study area. Two distinct growth patterns were found in the study area: bimodal and unimodal. These different growing patterns are mainly determined by the precipitation patterns. Besides the number of growing seasons, the other phenological characteristics also vary spatially because of the various precipitation patterns in East Africa. For example, earlier rainy season will result in earlier start of growing season, and the longer rainy season will correspond to a longer growing season. But even under the same

climatic conditions, phenology patterns vary due to different land cover types. For example, the grasslands tend to have shorter growing seasons compared with woodlands.

Significant changes in phenology from 1982 to 2006 have been observed in some places of the study area. For example, start of growing season has advanced in central Uganda while the start date has delayed in most places of Tanzania. There are also delayed end of growing season in Tanzania but earlier end dates in central Uganda. Shorter growing seasons have been found in parts of Tanzania while northern Uganda is having longer growing seasons. In addition, the magnitudes of changes are also not equal spatially due to different external forces and internal responses. For instance, the start of growing season has delayed by less than 1.5 days per year in central Tanzania while more than 1.5 days in eastern Tanzania. The growing season was shrunk by less than 2 days per year in central Tanzania while more than 2 days in northern Tanzania. Moreover, the changes are spatially heterogeneous. Most significant changes were found at croplands and woodlands in Uganda and Tanzania while grasslands in Kenya did not show many changes. The spatial heterogeneity is highly due to the spatial variations of changes in climate and land use/cover.

From 1982 to 2006, the precipitation pattern has changed. Local people in Tanzania have reported the later onset of rainy season, shorter rainy season, and rainfall comes in forms of several heavy rains. The annual rainfall is decreasing in southeast Tanzania based on CRU data. In Kenya, the short rains are becoming more and more irregular. Meanwhile, land use/cover is also changing because of economic development and increasing population. Human activities, including various cultivations, livestock grazing, and construction, have gradually modified the land surface. Major land use/cover changes are conversions from natural forest or savanna to crop lands and grazing lands. These changes from both climatic and anthropogenic factors were

main contributors to the phenological changes. However, the degrees of influences from two aspects are different from place to place. Climatic factor was found to be dominant in places where precipitation pattern has changed while no dramatic land cover changes were found, such as Tarangire national park in Tanzania and woodlands in south east Tanzania. The phenology and precipitation are highly correlated in these places while the residual may come from errors and land cover changes. On the other hand, anthropogenic factor was recognized as a dominating force of observed phenological changes in heavily agricultural and grazing areas, such as crop lands in central Tanzania and Uganda. In these places, there is no strong correlation between phenology and precipitation, while at the same time substantial land use/cover changes are detected.

Many limitations and challenges still exist and further investigations are needed. Firstly, the validation of phenology results remains a problem. Although the comparisons between the phenology and precipitation patterns can work as indirect validations, ground truth data about phenology is needed. Secondly, CRU rainfall data is used to present rainfall pattern and changes at regional scale as station data is not suitable for large scale analysis. However, CRU data is not reliable in East Africa because there is not enough station data when gridding. Therefore, one should be careful in drawing conclusions from CRU data. Thirdly, validation of land cover changes is very necessary. For example, the comparison of two different dataset, IGBP and MOD12Q1, showed some land use/cover changes. However, these changes could be due to ambiguity in the class definitions, or error during their classification. Additionally, the accuracy of classification based on Landsat data is not examined in this thesis because ground truth data is missing. These validation problems need to be solved in the future. Fourthly, only land use/cover change was examined considering anthropogenic factor. However, other influences, like actual

crop management which can affect the crop phenology substantially, were not addressed in this research.

REFERENCES

REFERENCES

- Aurela, M., T. Laurila, and J. P. Tuovinen. 2001. Seasonal CO₂ balances of a subarctic mire. *Journal of Geophysical Research-Atmospheres* 106 (D2):1623-1637.
- Badeck, F. W., A. Bondeau, K. Böttcher, D. Doktor, W. Lucht, J. Schaber, and S. Sitch. 2004. Responses of spring phenology to climate change. *New Phytologist* 162 (2):295-309.
- Beaubien, E. G., and H. J. Freeland. 2000. Spring phenology trends in Alberta, Canada: links to ocean temperature. *International Journal of Biometeorology* 44 (2):53-59.
- Bond, W. J., and G. F. Midgley. 2000. A proposed CO₂-controlled mechanism of woody plant invasion in grasslands and savannas. *Global Change Biology* 6 (8):865-869.
- Bond, W. J., G. F. Midgley, and F. I. Woodward. 2003. The importance of low atmospheric CO₂ and fire in promoting the spread of grasslands and savannas, 973-982: Blackwell Science Ltd.
- Boschetti, M., D. Stroppiana, P. A. Brivio, and S. Bocchi. 2009. Multi-year monitoring of rice crop phenology through time series analysis of MODIS images. *International Journal of Remote Sensing* 30 (18):4643-4662.
- Botta, A., N. Viovy, P. Ciais, P. Friedlingstein, and P. Monfray. 2000. A global prognostic scheme of leaf onset using satellite data. *Global Change Biology* 6 (7):709-725.
- Brooke, M. D., P. J. Jones, J. A. Vickery, and S. Waldren. 1996. Seasonal patterns of leaf growth and loss, flowering and fruiting on a subtropical Central Pacific island. *Biotropica* 28 (2):164-179.
- Casenave, A., and C. Valentin. 1992. A runoff capability classification system based on surface features criteria in semi-arid areas of West Africa. *Journal of Hydrology* 130 (1-4):231-249.
- Chen, X. Q., B. Hu, and R. Yu. 2005. Spatial and temporal variation of phenological growing season and climate change impacts in temperate eastern China. *Global Change Biology* 11 (7):1118-1130.
- Chen, X. Q., C. X. Xu, and Z. J. Tan. 2001. An analysis of relationships among plant community phenology and seasonal metrics of Normalized Difference Vegetation Index in the northern part of the monsoon region of China. *International Journal of Biometeorology* 45 (4):170-177.
- Chidumayo, E. N. 1994. Phenology and nutrition of miombo woodland trees in Zambia. *Trees-Structure and Function* 9 (2):67-72.

- Cleland, E. E., I. Chuine, A. Menzel, H. A. Mooney, and M. D. Schwartz. 2007. Shifting plant phenology in response to global change. *Trends in Ecology and Evolution* 22 (7):357-365.
- Corlett, R. T., and J. V. Lafrankie. 1998. Potential Impacts of Climate Change on Tropical Asian Forests Through an Influence on Phenology. *Climatic Change* 39 (2):439-453.
- Defila, C., and B. Clot. 2001. Phytophenological trends in Switzerland. *International Journal of Biometeorology* 45 (4):203-207.
- Despland, E., J. Rosenberg, and S. J. Simpson. 2004. Landscape structure and locust swarming: a satellite's eye view. *Ecography* 27 (3):381-391.
- Dingkuhn, M. 1995. Climatic determinants of irrigated rice performance in the Sahel. 3.Characterizing environments by simulating crop phenology. *Agricultural Systems* 48 (4):435-456.
- Dingkuhn, M., and F. Asch. 1999. Phenological responses of *Oryza sativa*, *O. glaberrima* and inter-specific rice cultivars on a toposequence in West Africa. *Euphytica* 110 (2):109-126.
- Dye, P. J., and B. H. Walker. 1987. Patterns of shoot growth in a semi-arid grassland in Zimbabwe. *Journal of Applied Ecology* 24 (2):633-644.
- Eklundh, L., and L. Olsson. 2003. Vegetation index trends for the African Sahel 1982-1999. *Geophysical Research Letters* 30 (8).
- Estrella, N., T. H. Sparks, and A. Menzel. 2007. Trends and temperature response in the phenology of crops in Germany. *Global Change Biology* 13 (8):1737-1747.
- Fenner, M. 1998. The phenology of growth and reproduction in plants *Perspectives in Plant Ecology, Evolution and Systematics* 1 (1):78 - 91.
- Foley, J. A., S. Levis, M. H. Costa, W. Cramer, and D. Pollard. 2000. Incorporating dynamic vegetation cover within global climate models. *Ecological Applications* 10 (6):1620-1632.
- Foley, J. A., I. C. Prentice, N. Ramankutty, S. Levis, D. Pollard, S. Sitch, and A. Haxeltine. 1996. An integrated biosphere model of land surface processes, terrestrial carbon balance, and vegetation dynamics. *Global Biogeochemical Cycles* 10 (4):603-628.
- Freedman, J. M., D. R. Fitzjarrald, K. E. Moore, and R. K. Sakai. 2001. Boundary layer clouds and vegetation-atmosphere feedbacks. *Journal of Climate* 14 (2):180-197.
- Fuller, D. O., and S. D. Prince. 1996. Rainfall and foliar dynamics in tropical southern Africa: Potential impacts of global climatic change on savanna vegetation. *Climatic Change* 33 (1):69-96.

- Funk, C., G. Senay, A. Asfaw, J. Verdin, J. Rowland, J. Michaelson, G. Eilerts, D. Korecha, and R. Choularton. 2005. Recent drought tendencies in Ethiopia and equatorial-subtropical eastern Africa. Washington DC, FEWS-NET.
- Heumann, B. W., J. W. Seaquist, L. Eklundh, and P. Jönsson. 2007. AVHRR derived phenological change in the Sahel and Soudan, Africa, 1982-2005. *Remote Sensing of Environment* 108 (4):385-392.
- Hickler, T., L. Eklundh, J. W. Seaquist, B. Smith, J. Ardo, L. Olsson, M. T. Sykes, and M. Sjöström. 2005. Precipitation controls Sahel greening trend. *Geophysical Research Letters* 32 (21).
- Hirsch, R. M., J. R. Slack, and R. A. Smith. 1982. Techniques of trend analysis for monthly water- quality data. *Water Resources Research* 18 (1):107-121.
- Holben, B. N. 1986. Characteristics of maximum-value composite images from temporal AVHRR data. *International Journal of Remote Sensing* 7 (11):1417-1434.
- Huete, A., K. Didan, T. Miura, E. P. Rodriguez, X. Gao, and L. G. Ferreira. 2002. Overview of the radiometric and biophysical performance of the MODIS vegetation indices. *Remote Sensing of Environment* 83 (1-2):195-213.
- Huete, A. R., H. Q. Liu, K. Batchily, and W. vanLeeuwen. 1997. A comparison of vegetation indices global set of TM images for EOS-MODIS. *Remote Sensing of Environment* 59 (3):440-451.
- Hulme, M., R. Doherty, T. Ngara, M. New, and D. Lister. 2001. African climate change: 1900-2100. *Climate Research* 17 (2):145-168.
- Hulme, P. E. 2005. Adapting to climate change: is there scope for ecological management in the face of a global threat? *Journal of Applied Ecology* 42 (5):784-794.
- Indeje, M., F. H. M. Semazzi, and L. J. Ogallo. 2000. ENSO signals in East African rainfall seasons. *International Journal of Climatology* 20 (1):19-46.
- IPCC, 2007: Climate Change 2007: The Physical Science Basis. Contribution of Working Group I to the Fourth Assessment Report of the Intergovernmental Panel on Climate Change [Solomon, S., D. Qin, M. Manning, Z. Chen, M. Marquis, K.B. Averyt, M. Tignor and H.L. Miller (eds.)]. Cambridge University Press, Cambridge, United Kingdom and New York, NY, USA.
- Jönsson, P., and L. Eklundh. 2002. Seasonality extraction by function fitting to time-series of satellite sensor data. *IEEE Transactions on Geoscience and Remote Sensing* 40 (8):1824-1832.

- Jönsson, P., and L. Eklundh. 2004. TIMESAT - a program for analyzing time-series of satellite sensor data. *Computers & Geosciences* 30 (8):833-845.
- Justice, C. O., J. R. G. Townshend, B. N. Holben, and C. J. Tucker. 1985. Analysis of the phenology of global vegetation using meteorological satellite data. *International Journal of Remote Sensing* 6 (8):1271-1318.
- Justice, C. O., E. Vermote, J. R. G. Townshend, R. Defries, D. P. Roy, D. K. Hall, V. V. Salomonson, J. L. Privette, G. Riggs, A. Strahler, W. Lucht, R. B. Myneni, Y. Knyazikhin, S. W. Running, R. R. Nemani, Z. M. Wan, A. R. Huete, W. van Leeuwen, R. E. Wolfe, L. Giglio, J. P. Muller, P. Lewis, and M. J. Barnsley. 1998. The Moderate Resolution Imaging Spectroradiometer (MODIS): Land remote sensing for global change research. *Ieee Transactions on Geoscience and Remote Sensing* 36 (4):1228-1249.
- Kaduk, J., and M. Heimann. 1996. A prognostic phenology scheme for global terrestrial carbon cycle models. *Climate Research* 6 (1):1-19.
- Keeling, C. D., J. F. S. Chin, and T. P. Whorf. 1996. Increased activity of northern vegetation inferred from atmospheric CO₂ measurements. *Nature* 382 (6587):146-149.
- King, D. 2005. Climate change: the science and the policy. *Journal of Applied Ecology* 42 (5):779-783.
- Kramer, K., I. Leinonen, and D. Loustau. 2000. The importance of phenology for the evaluation of impact of climate change on growth of boreal, temperate and Mediterranean forests ecosystems: an overview. *International Journal of Biometeorology* 44 (2):67-75.
- Lafleur, P. M., N. T. Roulet, and S. W. Admiral. 2001. Annual cycle of CO₂ exchange at a bog peatland. *Journal of Geophysical Research-Atmospheres* 106 (D3):3071-3081.
- Latifovic, R., and D. Pouliot. 2007. Analysis of climate change impacts on lake ice phenology in Canada using the historical satellite data record. *Remote Sensing of Environment* 106 (4):492-507.
- Li, M., J. J. Qu, and X. J. Hao. 2010. Investigating phenological changes using MODIS vegetation indices in deciduous broadleaf forest over continental U.S. during 2000-2008. *Ecological Informatics* 5 (5):410-417.
- Lieberman, D., and M. Lieberman. 1984. The causes and consequences of synchronous flushing in a dry tropical forest. *Biotropica* 16 (3):193-201.
- Lieth, H. 1974. Phenology and seasonality modelling. 444s ed: Springer.
- Lloyd, D. 1990. A phenological classification of terrestrial vegetation cover using shortwave vegetation index imagery. *International Journal of Remote Sensing* 11 (12):2269-2279.

- Loveland, T. R., B. C. Reed, J. F. Brown, D. O. Ohlen, Z. Zhu, L. Yang, and J. W. Merchant. 2000. Development of a global land cover characteristics database and IGBP DISCover from 1 km AVHRR data. *International Journal of Remote Sensing* 21 (6-7):1303-1330.
- Maignan, F., F. M. Breon, C. Bacour, J. Demarty, and A. Poirson. 2008. Interannual vegetation phenology estimates from global AVHRR measurements - Comparison with in situ data and applications. *Remote Sensing of Environment* 112 (2):496-505.
- McClanahan, T. R., and T. P. Young. 1996. *East African ecosystems and their conservation*. New York, USA: Oxford University Press.
- Menzel, A. 2000. Trends in phenological phases in Europe between 1951 and 1996. *International Journal of Biometeorology* 44 (2):76-81.
- Menzel, A., T. H. Sparks, N. Estrella, E. Koch, and A. Aasa. 2006. European phenological response to climate change matches the warming pattern. *Global Change Biology* 12 (10):1969-1976.
- Mitchell, T. D., and P. D. Jones. 2005. An improved method of constructing a database of monthly climate observations and associated high-resolution grids. *International Journal of Climatology* 25 (6):693-712.
- Moulin, S., L. Kergoat, N. Viovy, and G. Dedieu. 1997. Global-Scale Assessment of Vegetation Phenology Using NOAA/AVHRR Satellite Measurements. *Journal of Climate* 10 (6):1154-1170.
- Myneni, R. B., C. D. Keeling, C. J. Tucker, G. Asrar, and R. R. Nemani. 1997. Increased plant growth in the northern high latitudes from 1981 to 1991. *Nature* 386 (6626):698 - 702.
- Mayaux, P., E. Bartholomé, A. Cabral, M. Cherlet, P. Defourny, A. Di Gregorio, O. Diallo, M. Massart, A. Nonguierma, J.-F. Pekel, C. Pretorius, C. Vancutsem, M. Vasconcelos. 2003. *The Land Cover Map for Africa in the Year 2000*. GLC2000 database, European Commission Joint Research Centre, 2003.
- Nicholson, S. E., and E. Kim. 1997. The relationship of the El Nino Southern oscillation to African rainfall. *International Journal of Climatology* 17 (2):117-135.
- Ogutu, J. O., H. P. Piepho, H. T. Dublin, N. Bhola, and R. S. Reid. 2008. El Nino-Southern Oscillation, rainfall, temperature and Normalized Difference Vegetation Index fluctuations in the Mara-Serengeti ecosystem. *African Journal of Ecology* 46 (2):132-143.
- Olsson, L., L. Eklundh, and J. Ardo. 2005. A recent greening of the Sahel - Trends, patterns and potential causes. *Journal of Arid Environments* 63 (3):556-566.
- Parmesan, C., and G. Yohe. 2003. A globally coherent fingerprint of climate change impacts across natural systems. *Nature* 421 (6918):37-42.

- Partanen, J., V. Koski, and H. Hanninen. 1998. Effects of photoperiod and temperature on the timing of bud burst in Norway spruce (*Picea abies*). *Tree Physiology* 18 (12):811-816.
- Peñuelas, J., T. Rutishauser, and I. Filella. 2009. Phenology Feedbacks on Climate Change. *Science* 324 (5929):887-888.
- Pinzon, J., M.E. Brown, and C.J. Tucker. 2005. Satellite time series correction of orbital drift artifacts using empirical mode decomposition. In: N. Huang (Editor), *Hilbert-Huang Transform: Introduction and Applications*, pp. 167-186. .
- Prince, S. D., and C. J. Tucker. 1986. Satellite remote sensing of rangelands in Botswana II. NOAA AVHRR and herbaceous vegetation. *International Journal of Remote Sensing* 7 (11):1555-1570.
- Prins, H. H. T. 1988. Plant phenology patterns in Lake Manyara National Park, Tanzania. *Journal of Biogeography* 15 (3):465-480.
- Reed, B. C., J. F. Brown, D. Vanderzee, T. R. Loveland, J. W. Merchant, and D. O. Ohlen. 1994. Measuring Phenological Variability from Satellite Imagery. *Journal of Vegetation Science* 5 (5):703-714.
- Reich, P. B. 1995. Phenology of tropical forests: patterns, causes, and consequences. *Canadian Journal of Botany-Revue Canadienne De Botanique* 73 (2):164-174.
- Rietkerk, M., P. Ketner, J. Burger, B. Hoorens, and H. Olff. 2000. Multiscale soil and vegetation patchiness along a gradient of herbivore impact in a semi-arid grazing system in West Africa. *Plant Ecology* 148 (2):207-224.
- Rodriguez-Iturbe, I., P. D'Odorico, A. Porporato, and L. Ridolfi. 1999. On the spatial and temporal links between vegetation, climate, and soil moisture. *Water Resources Research* 35 (12):3709-3722.
- Rodriguez-Iturbe, I., P. D'Odorico, A. Porporato, and L. Ridolfi. 1999. Tree-grass coexistence in savannas: The role of spatial dynamics and climate fluctuations. *Geophysical Research Letters* 26 (2):247-250.
- Roetzer, T., M. Wittenzeller, H. Haeckel, and J. Nekovar. 2000. Phenology in central Europe - differences and trends of spring phenophases in urban and rural areas. *International Journal of Biometeorology* 44 (2):60-66.
- Root, T. L., J. T. Price, K. R. Hall, S. H. Schneider, C. Rosenzweig, and J. A. Pounds. 2003. Fingerprints of global warming on wild animals and plants. *Nature* 421 (6918):57-60.
- Scanlon, T. M., J. D. Albertson, K. K. Caylor, and C. A. Williams. 2002. Determining land surface fractional cover from NDVI and rainfall time series for a savanna ecosystem. *Remote Sensing of Environment* 82 (2-3):376-388.

- Schreck, C. J., and F. H. M. Semazzi. 2004. Variability of the recent climate of eastern Africa. *International Journal of Climatology* 24 (6):681-701.
- Schwartz, M. D. 1998. Green-wave phenology. *Nature* 394 (6696):839-840.
- Schwartz, M. D., R. Ahas, and A. Aasa. 2006. Onset of spring starting earlier across the Northern Hemisphere. *Global Change Biology* 12 (2):343-351.
- Sequist, J. W., L. Olsson, J. Ardo, and L. Eklundh. 2006. Broad-scale increase in NPP quantified for the African Sahel, 1982-1999. *International Journal of Remote Sensing* 27 (22):5115-5122.
- Sellers, P. J., C. J. Tucker, G. J. Collatz, S. O. Los, C. O. Justice, D. A. Dazlich, and D. A. Randall. 1994. A global 1 degree by 1 degree NDVI data set for climate studies. Part 2: The generation of global fields of terrestrial biophysical parameters from the NDVI. *International Journal of Remote Sensing* 15 (17):3519 - 3545.
- Sen, P. K. 1968. Estimates of the Regression Coefficient Based on Kendall's Tau. *Journal of the American Statistical Association* 63 (324):1379-1389.
- Stockli, R., and P. L. Vidale. 2004. European plant phenology and climate as seen in a 20-year AVHRR land-surface parameter dataset. *International Journal of Remote Sensing* 25 (17):3303-3330.
- Studer, S., R. Stockli, C. Appenzeller, and P. L. Vidale. 2007. A comparative study of satellite and ground-based phenology. *International Journal of Biometeorology* 51 (5):405-414.
- Trenberth, K. E., A. Dai, R. M. Rasmussen, and D. B. Parsons. 2003. The changing character of precipitation. *Bulletin of the American Meteorological Society* 84 (9):1205-+.
- Tucker, C. J., J.E. Pinzon, and M.E. Brown. 2004. Global Inventory Modeling and Mapping Studies, NA94apr15b.n11-VIg, 2.0, Global Land Cover Facility, University of Maryland, College Park, Maryland.
- Tucker, C. J., J. E. Pinzon, M. E. Brown, D. A. Slayback, E. W. Pak, R. Mahoney, E. F. Vermote, and N. El Saleous. 2005. An extended AVHRR 8-km NDVI dataset compatible with MODIS and SPOT vegetation NDVI data. *International Journal of Remote Sensing* 26 (20):4485-4498.
- White, M. A., S. W. Running, and P. E. Thornton. 1999. The impact of growing-season length variability on carbon assimilation and evapotranspiration over 88 years in the eastern US deciduous forest. *International Journal of Biometeorology* 42 (3):139-145.

- White, M. A., P. E. Thornton, and S. W. Running. 1997. A continental phenology model for monitoring vegetation responses to interannual climatic variability. *Global Biogeochemical Cycles* 11 (2):217-234.
- Wright, S. J., and C. P. Vanschaik. 1994. Light and the phenology of tropical trees. *American Naturalist* 143 (1):192-199.
- Xu, Z. X., J. Y. Li, and C. M. Liu. 2007. Long-term trend analysis for major climate variables in the Yellow River basin. *Hydrological Processes* 21 (14):1935-1948.
- Yang, L. H., and V. H. W. Rudolf. 2010. Phenology, ontogeny and the effects of climate change on the timing of species interactions. *Ecology Letters* 13 (1):1-10.
- Zhang, X. Y., M. A. Friedl, C. B. Schaaf, and A. H. Strahler. 2004. Climate controls on vegetation phenological patterns in northern mid- and high latitudes inferred from MODIS data. *Global Change Biology* 10 (7):1133-1145.
- Zhang, X. Y., M. A. Friedl, C. B. Schaaf, A. H. Strahler, J. C. F. Hodges, F. Gao, B. C. Reed, and A. Huete. 2003. Monitoring vegetation phenology using MODIS. *Remote Sensing of Environment* 84 (3):471-475.
- Zhang, X. Y., M. A. Friedl, C. B. Schaaf, A. H. Strahler, and Z. Liu. 2005. Monitoring the response of vegetation phenology to precipitation in Africa by coupling MODIS and TRMM instruments. *Journal of Geophysical Research-Atmospheres* 110 (D12).
- Zhou, L. M., C. J. Tucker, R. K. Kaufmann, D. Slayback, N. V. Shabanov, and R. B. Myneni. 2001. Variations in northern vegetation activity inferred from satellite data of vegetation index during 1981 to 1999. *Journal of Geophysical Research-Atmospheres* 106 (D17):20069-20083.
- Zoffoli, M. L., P. Kandus, N. Madanes, and D. H. Calvo. 2008. Seasonal and interannual analysis of wetlands in South America using NOAA-AVHRR NDVI time series: the case of the Parana Delta Region. *Landscape Ecology* 23 (7):833-848.